

# UNPAIRED MULTI-DOMAIN CAUSAL REPRESENTATION LEARNING

NILS STURMA<sup>1,2</sup>, CHANDLER SQUIRES<sup>2,3</sup>, MATHIAS DRTON<sup>1</sup>,  
AND CAROLINE UHLER<sup>2,3</sup>

**ABSTRACT.** The goal of causal representation learning is to find a representation of data that consists of causally related latent variables. We consider a setup where one has access to data from multiple domains that potentially share a causal representation. Crucially, observations in different domains are assumed to be unpaired, that is, we only observe the marginal distribution in each domain but not their joint distribution. In this paper, we give sufficient conditions for identifiability of the joint distribution and the shared causal graph in a linear setup. Identifiability holds if we can uniquely recover the joint distribution and the shared causal representation from the marginal distributions in each domain. We transform our identifiability results into a practical method to recover the shared latent causal graph. Moreover, we study how multiple domains reduce errors in falsely detecting shared causal variables in the finite data setting.

## 1. INTRODUCTION

An important challenge in machine learning is the integration and translation of data across multiple domains (Zhu et al., 2017; Zhuang et al., 2021). Researchers often have access to large amounts of unpaired data from several domains, e.g., images and text. It is then desirable to learn a probabilistic coupling between the observed marginal distributions that captures the relationship between the domains. One approach to tackle this problem is to assume that there is a latent representation that is invariant across the different domains (Bengio et al., 2013; Ericsson et al., 2022). Finding a probabilistic coupling then boils down to learning such a latent representation, that is, learning high-level, latent variables that explain the variation of the data within each domain as well as similarities across domains.

In traditional representation learning, the latent variables are assumed to be statistically independent, see for example the literature on independent component analysis (Hyvärinen and Oja, 2000; Comon and Jutten, 2010; Khemakhem et al., 2020). However, the assumption of independence can be too stringent and a poor match to reality. For example, the presence of clouds and the presence of wet roads in an image may be dependent, since clouds may cause rain which may in

<sup>1</sup>TECHNICAL UNIVERSITY OF MUNICH; TUM SCHOOL OF COMPUTATION, INFORMATION AND TECHNOLOGY, DEPARTMENT OF MATHEMATICS; MUNICH DATA SCIENCE INSTITUTE (MDSI); MUNICH CENTER FOR MACHINE LEARNING (MCML)

<sup>2</sup>BROAD INSTITUTE OF MIT AND HARVARD; ERIC AND WENDY SCHMIDT CENTER

<sup>3</sup>MASSACHUSETTS INSTITUTE OF TECHNOLOGY (MIT); LABORATORY FOR INFORMATION AND DECISION SYSTEMS

*E-mail addresses:* nils.sturma@tum.de, csquires@mit.edu, mathias.drton@tum.de, cuhler@mit.edu.

*Key words and phrases.* Causality, graphical models, independent component analysis, linear structural equation models, representation learning, structure identifiability.

turn cause wet roads. Thus, it is natural to seek a *causal representation*, that is, a set of high-level *causal* variables and relations among them (Schölkopf et al., 2021; Yang et al., 2021b). Figure 1 illustrates the setup of multi-domain causal representation learning, where multiple domains provide different views on a shared causal representation.

Our motivation to study multi-domain causal representations comes, in particular, from single-cell data in biology. Given a population of cells, different technologies such as imaging and sequencing provide different views on the population. Crucially, since these technologies destroy the cells, the observations are uncoupled, i.e., a specific cell may either be used for imaging or sequencing but not both. The aim is to integrate the different views on the population to study the underlying causal mechanisms determining the observed features in various domains (Butler et al., 2018; Stuart et al., 2019; Liu et al., 2019; Yang et al., 2021a; Lopez et al., 2022; Gossi et al., 2022; Cao et al., 2022).

In this paper, we study identifiability of the shared causal representation, that is, its uniqueness in the infinite data limit. Taking on the same perspective as, for example, in Schölkopf et al. (2021) and Seigal et al. (2022), we assume that observed data is generated in two steps. First, the latent variables  $Z = (Z_i)_{i \in \mathcal{H}}$  are sampled from a distribution  $P_Z$ , where  $P_Z$  is determined by an unknown structural causal model among the latent variables. Then, in each domain  $e \in \{1, \dots, m\}$ , the observed vector  $X^e \in \mathbb{R}^{d_e}$  is the image of a subset of the latent variables under a domain-specific, injective mixing function  $g_e$ . That is,

$$X^e = g_e(Z_{S_e}),$$

where  $S_e \subseteq \mathcal{H}$  is a subset of indices. A priori, it is unknown whether a latent variable  $Z_i$  with  $i \in S_e$  is shared across domains or domain-specific. Moreover, we only observe the marginal distribution of each random vector  $X^e$ , but none of the joint distributions over pairs  $X^e, X^f$  for  $e \neq f$ . Said differently, observations across domains are unpaired. Assuming that the structural causal model among the latent variables as well as the mixing functions are linear, our main contributions are:

- (1) We lay out conditions under which we are able to identify the joint distribution of  $X^1, \dots, X^m$ .
- (2) We give additional conditions under which we can identify the causal structure among the shared latent variables.

In particular, identifiability of the joint distribution across domains enables data translation. That is, given observation  $x$  in domain  $e$ , translation to domain  $f$  can be achieved by computing  $\mathbb{E}[X_f | X_e = x]$ . Furthermore, identifying the causal structure among the shared latent variables lets us study the effect of interventions on the different domains.

Our proofs leverage the identifiability of linear independent component analysis (Comon, 1994; Hyvärinen and Oja, 2000; Eriksson and Koivunen, 2004; Mesters and Zwiernik, 2022) as well as recent results on causal discovery under measurement error (Xie et al., 2020; Chen et al., 2022; Xie et al., 2022; Huang et al., 2022). We emphasize that our focus in this paper lies on identifiability. Nevertheless, our proofs also suggest methods to learn the joint distribution as well as the shared causal graph from finite samples. We provide an algorithm for the noisy setting and, moreover, we analyze how the number of domains reduce uncertainty with respect to the learned representation.

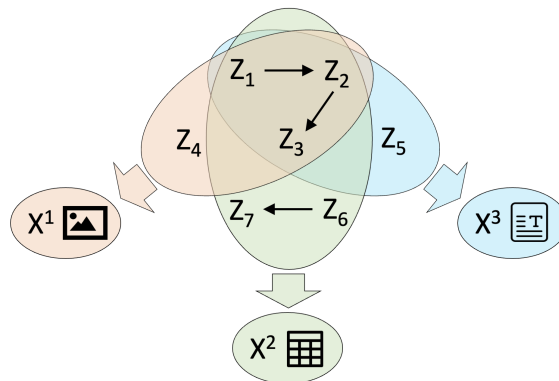


FIGURE 1. **Setup.** A latent causal representation where multiple domains  $X^e$  provide different “views” on subsets of the latent variables  $Z_i$ . The domains may correspond to different data modalities such as images, text or numerical data. Crucially, the observations across domains are unpaired, i.e., they arise from different states of the latent causal model.

The paper is organized as follows. In Section 1.1 we discuss further related work. Section 2 provides a precise definition of the considered setup. In Section 3 we study identifiability of the joint distribution and provide a method for learning the joint distribution from finite samples. We analyze how the method behaves with increasing number of domains. Using these results we study identifiability of the causal graph in Section 4. We conclude with a small simulation study as a proof of concept for the finite sample setting (Section 5). All technical proofs are deferred to the Appendix.

### 1.1. Related Work.

**Multi-domain Integration.** Motivated by technological developments for measuring different modalities at single-cell resolution, several methods have been proposed recently for domain translation between *unpaired* data. The proposed methods rely on a variety of techniques, including manifold alignment Welch et al. (2017); Amodio and Krishnaswamy (2018); Liu et al. (2019), matrix factorization (Duren et al., 2018), correlation analysis Barkas et al. (2019); Stuart et al. (2019), coupled autoencoders (Yang and Uhler, 2019), optimal transport (Cao et al., 2022), regression analysis (Yuan and Duren, 2022), and semisupervised learning (Lin et al., 2022). Implicitly, these methods presume the existence of a *shared* latent space where the different modalities either completely align or at least overlap. However, to the best of our knowledge, none of these methods have rigorous *identifiability* guarantees, i.e., the methods are not guaranteed to recover a correct domain translation mapping even for infinite data. Our work advances the theoretical understanding of multi-domain integration by providing identifiability guarantees on recovering the shared latent space.

**Group Independent Component Analysis.** The primary tool that we use for identifiability is linear independent component analysis (ICA) (Comon, 1994; Eriksson and Koivunen, 2004). Many works extend ICA to the multi-domain setting. These methods primarily come from computational neuroscience, where different domains correspond to different subjects or studies. However, to the best of our knowledge, all prior works require pairing between samples. These works can be categorized based on whether the samples are assumed to be voxels (Calhoun et al., 2001; Esposito et al., 2005), time points (Svensén et al., 2002; Varoquaux et al., 2009; Hyvärinen and Ramkumar, 2013), or either (Beckmann and Smith, 2005; Sui et al., 2009). For reviews, see Calhoun et al. (2009); Chabriel et al. (2014). Related are methods for *independent vector analysis* (Kim et al., 2006; Anderson et al., 2014; Bhinge et al., 2019) and multiset canonical correlation analysis (Nielsen, 2002; Li et al., 2011; Klami et al., 2014), which allow the latent variables to take on different values in each domain but still require sample pairing.

Most of the mentioned methods lack identifiability guarantees, only newer work (Richard et al., 2021) provides sufficient conditions for identifiability. Furthermore, all mentioned methods assume that every latent variable is shared across all domains. Other methods, e.g., Lukic et al. (2002) Maneshi et al. (2016), and Pandeva and Forré (2022), permit both shared and domain-specific components, but only consider the paired setting. In this paper, we extend these results to the *unpaired* setting.

**Latent Structure Discovery.** Learning causal structure between latent variables has a long history, e.g., in measurement models (Silva et al., 2006). One recent line of work studies the problem under the assumption of access to interventional data (e.g., Liu et al., 2022; Seigal et al., 2022). In particular, Seigal et al. (2022) show that the latent graph is identifiable if the interventions are sufficiently diverse. Another line of work shows that the graph is identified under certain sparsity assumptions on the mixing functions (Xie et al., 2020; Chen et al., 2022; Xie et al., 2022; Huang et al., 2022). We follow the second approach, that is, we will assume similar sparsity conditions on the mixing function and do not require interventional data.

## 1.2. Notation.

Let  $\mathbb{N}$  be the set of nonnegative integers. For positive  $n \in \mathbb{N}$ , we define  $[n] = \{1, \dots, n\}$ . For a matrix  $M \in \mathbb{R}^{a \times b}$ , we denote by  $M_{A,B}$  the submatrix containing the rows indexed by  $A \subseteq [a]$  and the columns indexed by  $B \subseteq [b]$ . Moreover, we write  $M_B$  for the submatrix containing all rows but only the subset of columns indexed by  $B$ . Similarly, for a tuple  $x = (x_1, \dots, x_b)$ , we denote by  $x_B$  the tuple only containing the entries indexed by  $B$ . A matrix  $Q = Q_\sigma \in \mathbb{R}^{p \times p}$  is a *signed permutation matrix* if it can be written as the product of a diagonal matrix  $D$  with entries  $D_{ii} \in \{\pm 1\}$  and a permutation matrix  $\tilde{Q}_\sigma$  with entries  $(\tilde{Q}_\sigma)_{ij} = \mathbb{1}_{j=\sigma(i)}$ , where  $\sigma$  is a permutation on  $p$  elements. Let  $P$  be a  $p$ -dimensional joint probability measure of a collection of random variables  $Y_1, \dots, Y_p$ . Then we denote by  $P_i$  the marginal probability measure such that  $Y_i \sim P_i$ . We say that  $P$  has *independent marginals* if the random variables  $Y_i$  are mutually independent. Moreover, we denote by  $M\#P$  the  $d$ -dimensional *push-forward measure* under the linear map defined by the matrix  $M \in \mathbb{R}^{d \times p}$ . If  $Q$  is a signed permutation matrix and the probability

measure  $P$  has independent marginals, then  $Q\#P$  also has independent marginals. For univariate probability measures we use the shorthand  $(-1)\#P = -P$ .

## 2. SETUP

Let  $\mathcal{H} = [h]$  for  $h \geq 1$ , and let  $Z = (Z_1, \dots, Z_h)$  be latent random variables that follow a linear structural equation model. That is, the variables are related by a linear equation

$$(1) \quad Z = AZ + \varepsilon,$$

with  $h \times h$  parameter matrix  $A = (a_{ij})$  and zero-mean, independent random variables  $\varepsilon = (\varepsilon_1, \dots, \varepsilon_h)$  that represent stochastic errors. Assume that we have observed random vectors  $X^e \in \mathbb{R}^{d_e}$  in multiple domains of interest  $e \in [m]$ , where the dimension  $d_e$  may vary across domains. Each random vector is the image under a linear function of a subset of the latent variables. In particular, we assume that there is a subset  $\mathcal{L} \subseteq \mathcal{H}$  representing the shared latent space such that each  $X^e$  is generated via the mechanism

$$(2) \quad X^e = G^e \cdot \begin{pmatrix} Z_{\mathcal{L}} \\ Z_{I_e} \end{pmatrix},$$

where  $I_e \subseteq \mathcal{H} \setminus \mathcal{L}$ . We say that the latent variable  $Z_{I_e}$  are *domain-specific* for domain  $e \in [m]$  while the latent variables  $Z_{\mathcal{L}}$  are *shared* across all domains. As already noted, we are motivated by settings where the shared latent variables  $Z_{\mathcal{L}}$  capture the key causal relations and the different domains are able to give us combined information about these relations. Likewise, we may think about the domain-specific latent variables  $Z_{I_e}$  as “noise” in each domain, independent of the shared latent variables. Specific models are now derived from (1)-(2) by assuming specific (but unknown) sparsity patterns in  $A$  and  $G^e$ . Each model is given by a “large” directed acyclic graph (DAG) that encodes the multi-domain setup. To formalize this, we introduce pairwise disjoint index sets  $V_1, \dots, V_m$ , where  $V_e$  indexes the coordinates of  $X^e$ , i.e.,  $X^e = (X_v : v \in V_e)$  and  $|V_e| = d_e$ . Then  $V = V_1 \cup \dots \cup V_m$  indexes all observed random variables. We define an  $m$ -domain graph such that the latent nodes are the only parents of observed nodes and there are no edges between shared and domain-specific latent nodes.

**Definition 2.1.** Let  $\mathcal{G}$  be a DAG whose vertex set is the disjoint union  $\mathcal{H} \cup V = \mathcal{H} \cup V_1 \cup \dots \cup V_m$ . Let  $D$  be the edge set of  $\mathcal{G}$ . Then  $\mathcal{G}$  is an  *$m$ -domain graph* with *shared latent nodes*  $\mathcal{L} = [\ell] \subseteq \mathcal{H}$  if the following is satisfied:

- (1) All parent sets contain only latent variables, i.e.,  $\text{pa}(v) = \{w : w \rightarrow v \in D\} \subseteq \mathcal{H}$  for all  $v \in \mathcal{H} \cup V$ .
- (2) The set  $\mathcal{L}$  consists of the common parents of variables in different domains, i.e.,  $u \in \mathcal{L}$  if and only if  $u \in \text{pa}(v) \cap \text{pa}(w)$  for  $v \in V_e, w \in V_f$  with  $e \neq f$ .
- (3) Let  $I_e = S_e \setminus \mathcal{L}$  be the domain-specific latent nodes, where  $S_e := \text{pa}(V_e) = \cup_{v \in V_e} \text{pa}(v) \subseteq \mathcal{H}$ . Then there are no edges in  $D$  that connect a node in  $\mathcal{L}$  and a node  $\cup_{e=1}^m I_e$  or that connect a node in  $I_e$  and a node in  $I_f$  for any  $e \neq f$ .

To emphasize that a given DAG is an  $m$ -domain graph we write  $\mathcal{G}_m$  instead of  $\mathcal{G}$ . We also say that  $S_e$  is the set of *latent parents* in domain  $e$  and denote its cardinality by  $s_e = |S_e|$ . Note that the third condition in Definition 2.1 does not

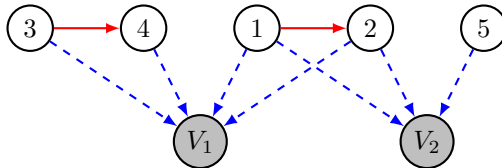


FIGURE 2. **Compact version of a 2-domain graph**  $\mathcal{G}_2$  with five latent nodes and two domains  $V_1$  and  $V_2$ . All observed nodes in each domain are represented by a single grey node. We draw a dashed blue edge from latent node  $h \in \mathcal{H}$  to domain  $V_e \subseteq V$  if  $h \in S_e = \text{pa}(V_e)$ . The random vectors associated to the two domains are uncoupled, that is, we do not observe their joint distribution.

exclude causal relations between the domain-specific latent variables, that is, there may be edges  $v \rightarrow w$  for  $v, w \in I_e$ . Since the sets  $I_e$  satisfy  $I_e \cap I_f = \emptyset$  for  $e \neq f$ , we specify w.l.o.g. the indexing convention  $I_e = \{\ell + 1 + \sum_{i=1}^{e-1} |I_i|, \dots, \ell + \sum_{i=1}^e |I_i|\}$  and  $h = \ell + \sum_{e=1}^m I_e$ .

**Example 2.2.** Consider the compact version of a 2-domain graph in Figure 2. There are  $h = 5$  latent nodes where  $\mathcal{L} = \{1, 2\}$  are shared and  $I_1 = \{3, 4\}$  and  $I_2 = \{5\}$  are domain-specific. A full  $m$ -domain graph is given in Appendix B.

Each  $m$ -domain graph postulates a statistical model that corresponds to the structural equation model in (1) and the mechanisms in (2), with potentially sparse matrices  $A$  and  $G^e$ . For two sets of nodes  $W, Y \subseteq \mathcal{H} \cup V$ , we denote by  $D_{WY}$  the subset of edges  $D_{WY} = \{y \rightarrow w \in D : w \in W, y \in Y\}$ . Moreover, let  $\mathbb{R}^{D_{WY}}$  be the set of real  $|W| \times |Y|$  matrices  $M = (m_{wy})$  with rows indexed by  $W$  and columns indexed by  $Y$ , such that the support is given by  $D_{WY}$ , that is,  $m_{wy} = 0$  if  $y \rightarrow w \notin D_{WY}$ .

**Definition 2.3.** Let  $\mathcal{G}_m = (\mathcal{H} \cup V, D)$  be an  $m$ -domain graph. Define the map

$$\begin{aligned} \phi_{\mathcal{G}_m} : \mathbb{R}^{D_{V\mathcal{H}}} \times \mathbb{R}^{D_{\mathcal{H}\mathcal{H}}} &\longrightarrow \mathbb{R}^{|\mathcal{H}| \times |\mathcal{H}|} \\ (G, A) &\longmapsto G \cdot (I - A)^{-1}. \end{aligned}$$

Then the *multi-domain causal representation (MDCR) model*  $\mathcal{M}(\mathcal{G}_m)$  is given by the set of probability measures  $P_X = B\#P$ , where  $B \in \text{Im}(\phi_{\mathcal{G}_m})$  and  $P$  is an  $h$ -dimensional probability measure with independent, mean-zero marginals  $P_i, i \in \mathcal{H}$ . We say that the pair  $(B, P)$  is a *representation* of  $P_X \in \mathcal{M}(\mathcal{G}_m)$ .

Definition 2.3 corresponds to the model defined in Equations (1) and (2). If  $P_X \in \mathcal{M}(\mathcal{G}_m)$  with representation  $(B, P)$ , then  $P_X$  is the joint distribution of the observed domains  $X = (X^1, \dots, X^m)$ . The distribution of the random variables  $\varepsilon_i$  in Equation (1) is given by the marginals  $P_i$ . Moreover, for any matrix  $G \in \mathbb{R}^{D_{V\mathcal{H}}}$ , we denote the submatrix  $G^e = G_{V_e, S_e} \in \mathbb{R}^{d_e \times s_e}$  which coincides with the matrix  $G^e$  from Equation (2). For the graph in Figure 2, we compute a concrete example of the matrix  $B$  in Example B.1 in the Appendix. Importantly, in the rest of the paper we assume to only observe the marginal distribution  $P_{X^e}$  in each domain but not the joint distribution  $P_X$ .

Ultimately, we are interested in recovering the graph  $G_{\mathcal{L}} = (\mathcal{L}, D_{\mathcal{L}\mathcal{L}})$  among the shared latent nodes. We proceed by a two-step approach: In Section 3 we recover the representation  $(B, P)$  of the joint distribution  $P_X$ . To be precise, we recover a matrix  $\widehat{B}$  that is equal to  $B$  up to certain permutations of the columns. Then we use the matrix  $\widehat{B}$  to recover the shared latent graph  $G_{\mathcal{L}}$  in Section 4 and show that recovery is possible up to trivial relabeling of latent nodes that appear in the same position of the causal order.

### 3. JOINT DISTRIBUTION

To identify the joint distribution  $P_X$ , we apply identifiability results from linear ICA in each domain separately and match the recovered probability measures  $P_i$  for identifying which of them are shared, that is, whether or not  $i \in \mathcal{L}$ .

#### 3.1. Main Identifiability Result.

Let  $\mathcal{G}_m$  be an  $m$ -domain graph with shared latent nodes  $\mathcal{L}$ , and let  $P_X \in \mathcal{M}(\mathcal{G}_m)$  with representation  $(B, P)$ . Recall that  $B = G(I - A)^{-1}$  with  $G \in \mathbb{R}^{D_V \times \mathcal{H}}$  and  $A \in \mathbb{R}^{D_{\mathcal{H}\mathcal{H}}}$ . We make the following technical assumptions to achieve identifiability.

- (C1) (Different error distributions.) The marginal distributions  $P_i, i \in \mathcal{H}$  are non-degenerate, non-symmetric and have unit variance. Moreover, the measures are pairwise different to each other and to the flipped versions, that is,  $P_i \neq P_j$  and  $P_i \neq -P_j$  for all  $i, j \in \mathcal{H}$  with  $i \neq j$ . Subsequently, we let  $d$  be a distance on the set of univariate Borel probability measures such that  $d(P_i, P_j) \neq 0$  and  $d(P_i, -P_j) \neq 0$  for  $i \neq j$ .
- (C2) (Full rank of mixing.) For each  $e \in [m]$ , the matrix  $G^e = G_{V_e, S_e} \in \mathbb{R}^{d_e \times s_e}$  is of full column rank.

Condition (C1) captures three aspects. First, by not allowing symmetric distributions, we assume in particular that the distributions of the errors are non-Gaussian. This allows for application of the results on identifiability of linear ICA. We discuss in Appendix C why non-Gaussianity is necessary to obtain identifiability of the joint distribution. Second, the genericity assumption that the error distributions are pairwise different allows for “matching” these distributions across domains to identify the ones corresponding to the shared latent space. Third, non-symmetric distributions account for the sign-indeterminacy of linear ICA for matching. Finally, Condition (C2) requires in particular that for each shared latent node  $k \in \mathcal{L}$  there is at least one node  $v \in V_e$  in every domain  $e \in [m]$  such that  $k \in \text{pa}(v)$ .

Under Conditions (C1) and (C2) we are able to derive a sufficient condition for identifiability of the joint distribution. Let  $SP(p)$  be the set of  $p \times p$  signed permutation matrices. We define the set of signed permutation *block matrices*:

$$\Pi = \left\{ \left( \begin{array}{cccc} \Psi_{\mathcal{L}} & & & \\ & \Psi_{I_1} & & \\ & & \ddots & \\ & & & \Psi_{I_m} \end{array} \right) : \begin{array}{l} \Psi_{\mathcal{L}} \in SP(\ell), \\ \Psi_{I_e} \in SP(|I_e|) \end{array} \right\}.$$

Our main result is the following.

**Algorithm 1** IdentifyJointDistribution

- 1: **Input:** Probability measures  $P_{X^e}$  for all  $e \in [m]$ .
- 2: **Output:** Number of shared latent variables  $\hat{\ell}$ , matrix  $\hat{B}$  and probability measure  $\hat{P}$  with independent marginals.
- 3: **for**  $e \in [m]$  **do**
- 4: Linear ICA: Find the smallest value  $\hat{s}_e$  such that  $P_{X^e} = \hat{B}^e \# P^e$  for a matrix  $\hat{B}^e \in \mathbb{R}^{d_e \times \hat{s}_e}$  and an  $\hat{s}_e$ -dimensional probability measure  $P^e$  with independent, mean-zero and unit-variance marginals  $P_i^e$ .
- 5: **end for**
- 6: Matching: Let  $\hat{\ell}$  be the maximal number such that there are signed permutation matrices  $\{Q^e\}_{e \in [m]}$  satisfying

$$d([(Q^e)^\top \# P^e]_i, [(Q^f)^\top \# P^f]_i) = 0$$

for all  $i = 1, \dots, \hat{\ell}$  and for all  $f \neq e$ .

- 7: Let  $\hat{\mathcal{L}} = \{1, \dots, \hat{\ell}\}$ .

- 8: Construct the matrix  $\hat{B}$  equal to

$$\left( \begin{array}{c|ccc} [\hat{B}^1 Q^1]_{\hat{\mathcal{L}}} & [\hat{B}^1 Q^1]_{[\hat{s}_1] \setminus \hat{\mathcal{L}}} & & \\ \vdots & & \ddots & \\ [\hat{B}^m Q^m]_{\hat{\mathcal{L}}} & & & [\hat{B}^m Q^m]_{[\hat{s}_m] \setminus \hat{\mathcal{L}}} \end{array} \right)$$

and the tuple of probability measures

$$\hat{P} = \left( \begin{array}{c} [(Q^1)^\top \# P^1]_{\hat{\mathcal{L}}} \\ [(Q^1)^\top \# P^1]_{[\hat{s}_1] \setminus \hat{\mathcal{L}}} \\ \vdots \\ [(Q^m)^\top \# P^m]_{[\hat{s}_m] \setminus \hat{\mathcal{L}}} \end{array} \right).$$

- 9: **return**  $(\hat{\ell}, \hat{B}, \hat{P})$ .

**Theorem 3.1.** *Let  $\mathcal{G}_m$  be an  $m$ -domain graph with shared latent nodes  $\mathcal{L} = [\ell]$ , and let  $P_X \in \mathcal{M}(\mathcal{G}_m)$  with representation  $(B, P)$ . Suppose that  $m \geq 2$  and that Conditions (C1) and (C2) are satisfied. Let  $(\hat{\ell}, \hat{B}, \hat{P})$  be the output of Algorithm 1. Then  $\hat{\ell} = \ell$  and*

$$\hat{B} = B \cdot \Psi \quad \text{and} \quad \hat{P} = \Psi^\top \# P,$$

for a signed permutation block matrix  $\Psi \in \Pi$ .

Theorem 3.1 says that the matrix  $B$  is identifiable up to signed block permutations of the columns. Under the assumptions of Theorem 3.1 it holds that  $\hat{B} \# \hat{P}$  is equal to  $P_X$ . That is, the joint distribution of the domains is identifiable.

*Remark 3.2.* By checking the proof of Theorem 3.1, the careful reader may notice that the statement of the theorem still holds true when we relax the third condition in the definition of an  $m$ -domain graph. That is, one may allow directed paths from shared to domain-specific latent nodes but not vice versa. For example, an additional edge  $1 \rightarrow 4$  between the latent nodes 1 and 4 would be allowed in the graph in Figure 2. In this case, the dependency structure of the domains is still determined by the shared latent space. However, the structural assumption that



there are no edges between shared and domain-specific latent nodes is made to obtain identifiability of the shared latent graph in Section 4.

### 3.2. Empirical Data.

We adjust Algorithm 1 such that it is applicable in the empirical data setting. That is, rather than the exact distribution  $P_{X^e}$ , we have a matrix of observations  $\mathbf{X}^e \in \mathbb{R}^{d_e \times n_e}$  in each domain  $e \in [m]$ . The sample size  $n_e$  might be different across domains. We denote  $n_{\min} = \min_{e \in [m]} n_e$  and  $n_{\max} = \max_{e \in [m]} n_e$ .

For implementing linear ICA on finite samples, multiple well developed algorithms are available, e.g., FastICA (Hyvärinen, 1999; Hyvärinen and Oja, 2000), Kernel ICA (Bach and Jordan, 2003) or JADE (Cardoso and Souloumiac, 1993). Applying them, we obtain a measure  $\hat{P}_i^e$  which is an estimator of the true measure  $P_i^e$  in Algorithm 1, Line 4.

The remaining challenge is the matching in Line 6 of Algorithm 1. For finite samples, the distance between empirical distributions is almost surely not zero although the true underlying distributions might be equal. In this section, we provide a matching strategy based on the two-sample Kolmogorov-Smirnov test (van der Vaart and Wellner, 1996, Section 3.7). We match two distributions if they are not significantly different. During this process, there might occur false discoveries, that is, distributions are matched that are actually not the same. We show that the probability of falsely discovering shared nodes shrinks exponentially with the number of domains.

For two univariate Borel probability measures  $P_i, P_j$ , with corresponding cumulative distribution functions  $F_i, F_j$ , the Kolmogorov-Smirnov distance is given by the  $L^\infty$ -distance

$$d_{\text{KS}}(P_i, P_j) = \|F_i - F_j\|_\infty = \sup_{x \in \mathbb{R}} |F_i(x) - F_j(x)|.$$

The two-sample Kolmogorov-Smirnov test statistic for the null hypothesis  $H_0 : d_{\text{KS}}(P_i^e, P_j^f) = 0$  is given by

$$(3) \quad T(\hat{P}_i^e, \hat{P}_j^f) = \sqrt{\frac{n_e n_f}{n_e + n_f}} d_{\text{KS}}(\hat{P}_i^e, \hat{P}_j^f).$$

It is important to note that  $\hat{P}_i^e$  is not an empirical measure in the classical sense since it is not obtained from data sampled directly from the true distribution  $P_i^e$ . In addition to the sampling error there is the uncertainty of the ICA algorithm. However, in the analysis we present here, we will neglect this error and treat  $\hat{P}_i^e$  as an empirical measure. In this case, under  $H_0$ , the test statistic  $T(\hat{P}_i^e, \hat{P}_j^f)$  converges in distribution to  $\|B\|_\infty$ , where  $B$  is a Brownian bridge from 0 to 1 (van der Vaart and Wellner, 1996). For a given level  $\alpha \in (0, 1)$ , we choose the critical value as  $c_\alpha = \inf\{t : P(\|B\|_\infty > t) \leq \alpha\}$  and reject  $H_0$  if  $T(\hat{P}_i^e, \hat{P}_j^f) > c_\alpha$ .

**Definition 3.3.** Let  $\alpha \in (0, 1)$  and suppose the distributions  $\{\hat{P}_1^e, \dots, \hat{P}_{s_e}^e\}$  and  $\{\hat{P}_1^f, \dots, \hat{P}_{s_f}^f\}$  are given for two domains  $e, f \in [m]$ . Define

$$\Omega_\alpha(\hat{P}_i^e, \hat{P}_j^f) = \begin{cases} 1 & \text{if } T_{ij}^{ef} \leq c_\alpha \text{ and } T_{ij}^{ef} = \min\{\min_{k \in [s_f]} T_{ik}^{ef}, \min_{k \in [s_e]} T_{kj}^{ef}\}, \\ 0 & \text{else,} \end{cases}$$

where  $T_{ij}^{ef} = \min\{T(\widehat{P}_i^e, \widehat{P}_j^f), T(\widehat{P}_i^e, -\widehat{P}_j^f)\}$ .

We say that  $\widehat{P}_i^e$  and  $\widehat{P}_j^f$  are *matched* if  $\Omega_\alpha(\widehat{P}_i^e, \widehat{P}_j^f) = 1$ .

Definition 3.3 essentially states that two measures are matched if the test statistic (3) is not significantly large and the null hypothesis cannot be rejected. Taking the minimum of  $T(\widehat{P}_i^e, \widehat{P}_j^f)$  and  $T(\widehat{P}_i^e, -\widehat{P}_j^f)$  accounts for the sign indeterminacy of linear ICA. For two fixed domains  $e, f \in [m]$ , if it happens that the statistic  $T_{ij}^{ef}$  for multiple pairs  $(i, j)$  is small enough, then the pair with the minimal value of the statistic is matched. Note that one may use any other test than the Kolmogorov-Smirnov test to define a matching as in Definition 3.3. We discover a shared latent node if it is matched consistently across domains.

**Definition 3.4.** Let  $C = (i_1, \dots, i_m)$  be a tuple with  $m$  elements such that  $i_e \in [\widehat{s}_e]$ . Then we say that  $C$  determines a *shared node* if  $\Omega_\alpha(\widehat{P}_{i_e}^e, \widehat{P}_{i_f}^f) = 1$  for all  $i_e, i_f \in C$ .

Inferring the existence of a shared node which does not actually exist may be considered a more serious error than inferring a shared node determined by a set  $C$ , where only some components of  $C$  are wrongly matched. In the following theorem we show that the probability of falsely discovering shared nodes shrinks exponentially with the number of wrongly matched components.

**Theorem 3.5.** Let  $C = (i_1, \dots, i_m)$  be a tuple with  $m$  elements such that  $i_e \in [\widehat{s}_e]$ . Let  $g : \mathbb{N} \times \mathbb{R}_{\geq 0} \rightarrow \mathbb{R}_{\geq 0}$  be a function that is monotonically decreasing in  $n \in \mathbb{N}$ . Assume the following conditions:

- (i)  $P(d_{KS}(\widehat{P}_{i_e}^e, P_{i_e}^e) > x) \leq g(n_e, x)$  for all  $e \in [m]$  and for all  $x \geq 0$ .
- (ii) There is  $E \subseteq [m]$  with  $|E| \geq 2$  and a constant  $\kappa > 0$  such that  $d_{KS}(P_{i_e}^e, P_{i_f}^f) \geq \kappa$  and  $d_{KS}(P_{i_e}^e, -P_{i_f}^f) \geq \kappa$  for all  $e \in E, f \in [m]$  with  $e \neq f$ .

Then

$$P(C \text{ determines a shared node}) \leq g\left(n_{\min}, \max\left\{\frac{\kappa}{2} - \frac{\sqrt{n_{\max}}}{\sqrt{2} n_{\min}} c_\alpha, 0\right\}\right)^{|E|-1}.$$

If  $\widehat{P}_i^e$  were an empirical measure in the classical sense, then Condition (i) in Theorem 3.5 translates to the well-known Dvoretzky–Kiefer–Wolfowitz inequality, that is, the function  $g$  is given by  $g(n, x) = 2 \exp(-2nx^2)$ . Given a tuple  $C = (i_1, \dots, i_m)$  that defines a shared node, Condition (ii) is an assumption on the number of wrongly matched components. The most extreme case is when the shared node does not actually exist and all components are wrongly matched. That is, the measures  $\widehat{P}_{i_e}^e$  and  $\widehat{P}_{i_f}^f$  are matched even though  $d_{KS}(P_{i_e}^e, P_{i_f}^f) \neq 0$  and  $d_{KS}(P_{i_e}^e, -P_{i_f}^f) \neq 0$  for all  $e, f \in [m]$ . On the other hand, if  $|E| \ll m$ , then  $C$  determines a shared node where the majority of the components are correctly matched.

If  $g(n, x) \rightarrow 0$  for  $n \rightarrow \infty$  and  $x > 0$ , the statement of the theorem becomes meaningful under the constraint  $\sqrt{n_{\max}}/n_{\min} \rightarrow \infty$ . In this case, the probability that a given tuple  $C$  with wrong components  $E$  determines a shared node goes to zero for large sample sizes  $n_{\min}$ . As noted, the probability of falsely discovering a shared node decreases exponentially with the number of wrongly matched components  $|E|$ . In the extreme case, this means that the probability of falsely discovering shared

nodes with all components wrongly matched, i.e.,  $E = [m]$ , decreases exponentially with the number of domains  $m$ .

Theorem 3.5 also tells us that the probability of falsely matching two measures  $\widehat{P}_i^e$  and  $\widehat{P}_j^f$  becomes zero if the sample size grows to infinity and the linear ICA algorithm is consistent. However, with finite samples we might fail to match two measures where the underlying true measures are actually the same, i.e., we falsely reject the true null hypothesis  $H_0$ . Thus, we might be overly conservative in detecting shared nodes due to a high family-wise error rate caused by multiple testing. We suggest to correct the level  $\alpha$  to account for the amount of tests carried out. One possibility is to apply a Bonferroni-type correction. The total number of tests is given by  $t = 2 \sum_{e < f} \widehat{s}_e \widehat{s}_f$ . This means that an adjusted level is given by  $\alpha_t = \alpha/t$  and instead of the critical value  $c_\alpha$  we consider the adjusted critical value  $c_{\alpha_t}$ . In Appendix D we state a complete version of Algorithm 1 for the finite sample setting.

#### 4. IDENTIFIABILITY OF THE CAUSAL GRAPH

We return to our goal of identifying the causal graph  $\mathcal{G}_\mathcal{L} = (\mathcal{L}, D_{\mathcal{L}\mathcal{L}})$  among the shared latent nodes. By Theorem 3.1, we can identify the representation  $(B, P)$  of  $P_X \in \mathcal{M}(\mathcal{G}_m)$  from the marginal distributions. In particular, we recover the matrix  $\widehat{B} = B\Psi$  for a signed permutation block matrix  $\Psi \in \Pi$ . Moreover, we know which columns correspond to the shared latent nodes. That is, we know that the submatrix  $\widehat{B}_\mathcal{L}$  obtained by only considering the columns indexed by  $\mathcal{L} = \widehat{\mathcal{L}} = [\ell]$  is equal to  $B_\mathcal{L}\Psi_\mathcal{L}$ , where  $\Psi_\mathcal{L} \in SP(\ell)$ .

**Problem 4.1.** Let  $B \in \text{Im}(\phi_{\mathcal{G}_m})$  for an  $m$ -domain graph  $\mathcal{G}_m$  with shared latent nodes  $\mathcal{L}$ . Given the matrix  $\widehat{B}_\mathcal{L} = B_\mathcal{L}\Psi_\mathcal{L}$  with  $\Psi_\mathcal{L}$  a signed permutation matrix, when is it possible to identify the causal graph  $\mathcal{G}_\mathcal{L}$ ?

Recently, Xie et al. (2022) and Dai et al. (2022) show that, in the one-domain setting with independent additive noise, the latent graph can be identified if each latent variable has at least two pure children. We obtain a comparable result.

**Definition 4.2.** Let  $\mathcal{G}_m = (\mathcal{H} \cup V, D)$  be an  $m$ -domain graph with shared latent nodes  $\mathcal{L} \subseteq \mathcal{H}$ . For a shared latent node  $k \in \mathcal{L}$ , we say that an observed node  $v \in V$  is a *partial pure child* of  $k$  if  $\text{pa}(v) \cap \mathcal{L} = \{k\}$ .

For a partial pure child  $v \in V$ , there may still be domain-specific latent nodes that are parents of  $v$ . Definition 4.2 only requires that there is exactly one parent that is in the set  $\mathcal{L}$ . This explains the name *partial* pure child; see Example B.2 in the Appendix for further elaboration.

W.l.o.g. we assume in this section that the shared latent nodes are *topologically ordered* such that  $i \rightarrow j \in D_{\mathcal{L}\mathcal{L}}$  implies  $i < j$  for all  $i, j \in \mathcal{L}$ . We further assume:

(C3) (Two partial pure children across domains.) For each shared latent node  $k \in \mathcal{L}$ , there exist two *partial pure children*.

(C4) (Rank faithfulness.) For any two subsets  $Y \subseteq V$  and  $W \subseteq \mathcal{L}$ , we assume that

$$\text{rank}(B_{Y,W}) = \max_{B' \in \text{Im}(\phi_{\mathcal{G}_m})} \text{rank}(B'_{Y,W}).$$

The two partial pure children required in Condition (C3) may either be in distinct domains or in a single domain. Roughly speaking, we assume in Condition (C4) that no configuration of edge parameters coincidentally yields low rank. The set of

**Algorithm 2** IdentifySharedGraph

- 
- 1: **Input:** Matrix  $B^* \in \mathbb{R}^{|V| \times \ell}$ .
  - 2: **Output:** Parameter matrix  $\hat{A} \in \mathbb{R}^{\ell \times \ell}$ .
  - 3: Remove rows  $B_{i, \mathcal{L}}^*$  from the matrix  $B^*$  that are completely zero.
  - 4: Find tuples  $(i_k, j_k)_{k \in \mathcal{L}}$  with  $i_k \neq j_k$  such that
    - (i)  $\text{rank}(B_{\{i_k, j_k\}, \mathcal{L}}^*) = 1$  for all  $k \in \mathcal{L}$  and
    - (ii)  $\text{rank}(B_{\{i_k, i_q\}, \mathcal{L}}^*) = 2$  for all  $k, q \in \mathcal{L}$  with  $k \neq q$ .
  - 5: Let  $I = \{i_1, \dots, i_\ell\}$  and consider  $B_{I, \mathcal{L}}^* \in \mathbb{R}^{\ell \times \ell}$ .
  - 6: Find two permutation matrices  $R_1$  and  $R_2$  such that  $W = R_1 B_{I, \mathcal{L}}^* R_2$  is lower triangular.
  - 7: Multiply each column of  $W$  by the sign of its corresponding diagonal element. This yields a new matrix  $\widetilde{W}$  with all diagonal elements positive.
  - 8: Divide each row of  $\widetilde{W}$  by its corresponding diagonal element. This yields a new matrix  $\widetilde{W}'$  with all diagonal elements equal to one.
  - 9: Compute  $\hat{A} = I - (\widetilde{W}')^{-1}$ .
  - 10: **return**  $\hat{A}$ .
- 

matrices  $B \in \text{Im}(\phi_{\mathcal{G}_m})$  that violates (C4) is a subset of measure zero of  $\text{Im}(\phi_{\mathcal{G}_m})$  with respect to the Lebesgue measure. Note that our conditions do not impose constraints on the graph  $\mathcal{G}_{\mathcal{L}}$ . Our main tool to tackle Problem 4.1 will be the following lemma.

**Lemma 4.3.** *Let  $B \in \text{Im}(\phi_{\mathcal{G}_m})$  for an  $m$ -domain graph  $\mathcal{G}_m$ . Suppose that Condition (C4) is satisfied and that there are no zero-rows in  $B_{\mathcal{L}}$ . Let  $v, w \in V$ . Then  $\text{rank}(B_{\{v, w\}, \mathcal{L}}) = 1$  if and only if there is a node  $k \in \mathcal{L}$  such that both  $v$  and  $w$  are partial pure children of  $k$ .*

The condition on no zero-rows in Lemma 4.3 is needed since we always have  $\text{rank}(B_{\{v, w\}, \mathcal{L}}) \leq 1$  if one of the two rows is zero. However, this is no additional structural assumption since we allow zero-rows when identifying the latent graph; c.f. Algorithm 2. The lemma allows us to find partial pure children by testing a rank constraint on the matrix  $\widehat{B}_{\mathcal{L}}$ . If  $(i_1, j_1)$  and  $(i_2, j_2)$  are partial pure children of two nodes in  $\mathcal{L}$ , we make sure that these two nodes are different by checking that  $\text{rank}(B_{\{i_1, i_2\}, \mathcal{L}}) = 2$ .

For a DAG  $G = (V, D)$ , we define  $\mathcal{S}(G)$  to be the set of permutations on  $|V|$  elements that are consistent with the DAG, i.e., such that  $\sigma(i) < \sigma(j)$  for all edges  $i \rightarrow j \in D$ . The following result is the main result of this section.

**Theorem 4.4.** *Let  $\widehat{B} = B\Psi$  with  $B \in \text{Im}(\phi_{\mathcal{G}_m})$  and  $\Psi \in \Pi$ , and define  $B^* = \widehat{B}_{\mathcal{L}}$  to be the input of Algorithm 2. Assume that Conditions (C3) and (C4) are satisfied, and let  $\hat{A}$  be the output of Algorithm 2. Then  $\hat{A} = Q_\sigma^\top A_{\mathcal{L}, \mathcal{L}} Q_\sigma$  for a signed permutation matrix  $Q_\sigma$  with  $\sigma \in \mathcal{S}(\mathcal{G}_{\mathcal{L}})$ . Moreover, if  $G_{vk} > 0$  for  $G \in \mathbb{R}^{D_{V \times \mathcal{L}}}$  whenever  $v$  is a pure child of  $k$ , then  $Q_\sigma$  is a permutation matrix.*

Theorem 4.4 states that the graph  $\mathcal{G}_{\mathcal{L}}$  can be uniquely recovered up to a permutation of the nodes that preserves the property that  $i \rightarrow j$  implies  $i < j$ ; see Remark 4.5. Since the columns of the matrix  $\widehat{B}$  are not only permuted but also of different signs, we solve the sign indeterminacy column-wise in Line 7 before removing the

scaling indeterminacy row-wise in Line 8. In case the coefficients corresponding to pure children are positive, this ensures that  $Q_\sigma$  is a *permutation matrix* and we have no sign indeterminacy.

*Remark 4.5.* Let  $\widehat{A}$  be the output of Algorithm 2. Then we construct the graph  $\widehat{G}_\mathcal{L} = (\mathcal{L}, \widehat{D}_{\mathcal{L}\mathcal{L}})$  as the graph with edges  $j \rightarrow i \in \widehat{D}_{\mathcal{L}\mathcal{L}}$  if and only if  $\widehat{A}_{ij} \neq 0$ . Condition (C4) ensures that  $\widehat{G}_\mathcal{L}$  is equivalent to  $\mathcal{G}_\mathcal{L}$  in the sense that there is a permutation  $\sigma \in \mathcal{S}(\mathcal{G}_\mathcal{L})$  such that  $\widehat{D}_{\mathcal{L}\mathcal{L}} = \{\sigma(i) \rightarrow \sigma(j) : i \rightarrow j \in D_{\mathcal{L}\mathcal{L}}\}$ .

In Appendix D we adapt Algorithm 2 for the empirical data setting, where we only have an approximation  $\widehat{B}_\mathcal{L} \approx B_\mathcal{L}\psi_\mathcal{L}$ .

## 5. SIMULATIONS

In this section we report on a small simulation study to illustrate the validity of our adapted algorithms for finite samples (detailed in Appendix D). We emphasize that this should only serve as a proof of concept as the focus of our work lies on the identifiability results. In potential future work one may develop more sophisticated methods; c.f. Appendix G. The adapted algorithms have a hyperparameter  $\gamma$ , which is a threshold on singular values to determine the rank of a matrix. In our simulations we use  $\gamma = 0.1$ .

### 5.1. Data Generation.

In each experiment we generate 1000 random models with  $\ell = 3$  shared latent nodes. We consider different numbers of domains  $m \in \{2, 3\}$  and assume that there are  $|I_e| = 2$  domain-specific latent nodes for each domain. The dimensions are given by  $d_e = d/m$  for all  $e \in [m]$  and  $d = 30$ . We sample the  $m$ -domain graph  $\mathcal{G}_m$  on the shared latent nodes as follows. First, we sample the graph  $\mathcal{G}_\mathcal{L}$  from an Erdős-Rényi model with edge probability 0.75 and assume that there are no edges between other latent nodes, that is, between  $\mathcal{L}$  and  $\mathcal{H} \setminus \mathcal{L}$  and within  $\mathcal{H} \setminus \mathcal{L}$ . Then we fix two partial pure children for each shared latent node  $k \in \mathcal{L}$  and collect them in the set  $W$ . The remaining edges from  $\mathcal{L}$  to  $V \setminus W$  and from  $\mathcal{H}$  to  $V$  are sampled from an Erdős-Rényi model with edge probability 0.9. Finally, the (nonzero) entries of  $G$  and  $A$  are sampled from  $\text{Unif}(\pm[0.25, 1])$ . The distributions of the error variables are specified in Appendix E. For simplicity, we assume that the sample sizes coincide, that is,  $n_e = n$  for all  $e \in [m]$ , and consider  $n \in \{1000, 2500, 5000, 10000, 25000\}$ .

### 5.2. Results.

First, we plot the average number of shared nodes  $\widehat{\ell}$  in our experiments in Figure 3 (a). Especially for low sample sizes, we see that fewer shared nodes are detected with more domains. However, we also plot the fraction of experiments where  $\widehat{\ell} > \ell$  in Figure 3 (b). We find that the percentage where  $\widehat{\ell} > \ell$  decreases drastically when considering 3 instead of 2 domains and is almost equal to zero already for  $m = 3$ . This suggests that the number of falsely detected shared nodes is very low, as expected by Theorem 3.5. Our findings show that more domains lead to a more conservative discovery of shared nodes, but whenever a shared node is determined this is more certain. Moreover, we measure the error in estimating  $\widehat{B}_\mathcal{L}$  in Figure 3

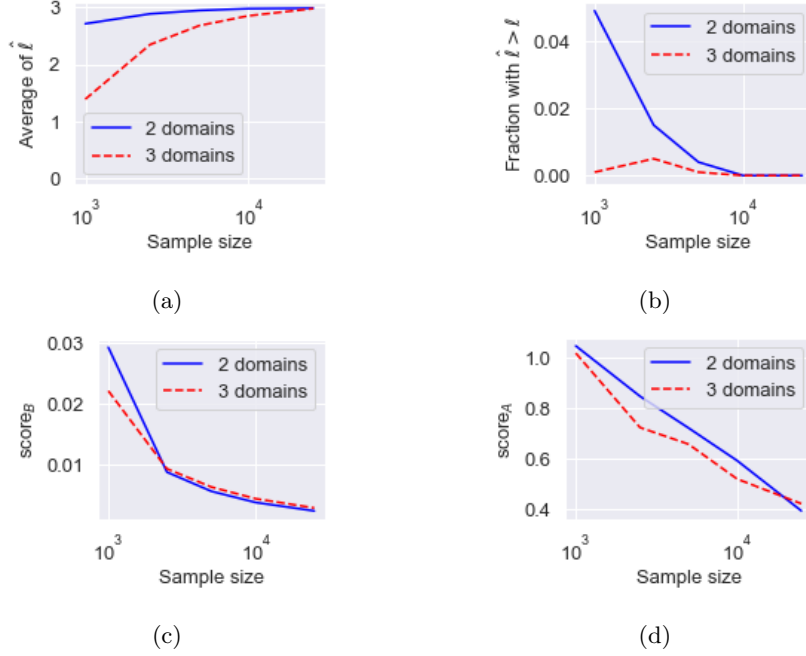


FIGURE 3. **Results.** Logarithmic scale on the  $x$ -axis.

(c), that is, the error in the “shared” columns. We take

$$\text{score}_B(\hat{B}_{\hat{\ell}}) = \begin{cases} \min_{\Psi \in SP(\ell)} \beta_{\ell, \hat{\ell}}^{-1/2} \|\hat{B}_{\hat{\ell}} - [B_{\mathcal{L}} \Psi]_{\hat{\ell}}\|_{\mathcal{F}} & \text{if } \hat{\ell} \leq \ell, \\ \min_{\Psi \in SP(\hat{\ell})} \beta_{\ell, \hat{\ell}}^{-1/2} \|[\hat{B}_{\hat{\ell}} \Psi]_{\mathcal{L}} - B_{\mathcal{L}}\|_{\mathcal{F}} & \text{if } \hat{\ell} > \ell, \end{cases}$$

where  $\|\cdot\|_{\mathcal{F}}$  denotes the Frobenius norm and  $\beta_{\ell, \hat{\ell}} = \min\{\ell, \hat{\ell}\} \cdot \sum_{e=1}^m d_e$  denotes the number of entries of the matrix over which the norm is taken. In the cases  $\ell = \hat{\ell}$ , we also measure the performance of recovering the shared latent graph  $\mathcal{G}_{\mathcal{L}}$  in Figure 3 (d) by taking

$$\text{score}_A(\hat{A}) = \min_{Q_{\sigma} \in SP(\ell) \text{ s.t. } \sigma \in S(\mathcal{G}_{\mathcal{L}})} \frac{1}{\ell} \|Q_{\sigma}^{\top} \hat{A} Q_{\sigma} - A_{\mathcal{L}, \mathcal{L}}\|_{\mathcal{F}}.$$

As expected, the estimation errors for  $B_{\mathcal{L}}$  and  $A_{\mathcal{L}, \mathcal{L}}$  decrease with increasing sample size. Additional simulation results with larger  $\ell$  can be found in Appendix F.

## 6. DISCUSSION

This work introduces the problem of causal representation learning from *unpaired* multi-domain observations, in which multiple domains provide complementary information about a set of shared latent nodes that are the causal quantities of primary interest. For this problem, we laid out a setting in which we can provably identify the causal relations among the shared latent nodes. To identify the desired causal structure, we proposed a two-step approach where we first make use of linear ICA in each domain separately and match the recovered error distributions to identify shared nodes and the joint distribution of the domains. In the second step, we identify

the causal structure among the shared latent variables by testing rank deficiencies in the “overall mixing matrix”  $B$ . To the best of our knowledge, our guarantees are the first principled identifiability results for shared causal representations in an unpaired multi-domain setting.

We proposed algorithms for recovering the joint distribution and the shared latent space making our proofs constructive. While our focus is on identifiability guarantees, we showed how our proofs give rise to algorithms for the finite sample setting. Moreover, we proposed a method to match approximate error distributions and showed that the probability of falsely discovering shared nodes decreases exponentially in the number of domains. Our work opens up numerous directions for future work as we discuss in Appendix G.

#### ACKNOWLEDGEMENTS

This project has received funding from the European Research Council (ERC) under the European Union’s Horizon 2020 research and innovation programme (grant agreement No 883818) to Mathias Drton as well as funding from NCCIH/NIH (1DP2AT012345), ONR (N00014-22-1-2116), NSF (DMS-1651995), the MIT-IBM Watson AI Lab, and a Simons Investigator Award to Caroline Uhler. Nils Sturma acknowledges support by the Munich Data Science Institute (MDSI) at Technical University of Munich (TUM) via the Linde/MDSI PhD Fellowship program. Chandler Squires was partially supported by an NSF Graduate Research Fellowship.

#### REFERENCES

- Amodio, M. and Krishnaswamy, S. (2018). MAGAN: Aligning biological manifolds. In Dy, J. and Krause, A., editors, *Proceedings of the 35th International Conference on Machine Learning*, volume 80 of *Proceedings of Machine Learning Research*, pages 215–223. PMLR.
- Anderson, M., Fu, G.-S., Phlypo, R., and Adalı, T. (2014). Independent vector analysis: Identification conditions and performance bounds. *IEEE Trans. Signal Process.*, 62(17):4399–4410.
- Bach, F. R. and Jordan, M. I. (2003). Kernel independent component analysis. *J. Mach. Learn. Res.*, 3(1):1–48.
- Barkas, N., Petukhov, V., Nikolaeva, D., Lozinsky, Y., Demharter, S., Khodosevich, K., and Kharchenko, P. V. (2019). Joint analysis of heterogeneous single-cell RNA-seq dataset collections. *Nat. Methods*, 16(8):695–698.
- Beckmann, C. F. and Smith, S. M. (2005). Tensorial extensions of independent component analysis for multisubject fMRI analysis. *Neuroimage*, 25(1):294–311.
- Bengio, Y., Courville, A., and Vincent, P. (2013). Representation learning: A review and new perspectives. *IEEE Trans. Pattern Anal. Mach. Intell.*, 35(8):1798–1828.
- Bhinge, S., Mowakeaa, R., Calhoun, V. D., and Adalı, T. (2019). Extraction of time-varying spatiotemporal networks using parameter-tuned constrained IVA. *IEEE Trans. Med. Imaging*, 38(7):1715–1725.
- Butler, A., Hoffman, P., Smibert, P., Papalexi, E., and Satija, R. (2018). Integrating single-cell transcriptomic data across different conditions, technologies, and species. *Nat. Biotechnol.*, 36(5):411–420.
- Calhoun, V. D., Adalı, T., Pearlson, G. D., and Pekar, J. J. (2001). A method for making group inferences from functional MRI data using independent component analysis. *Hum. Brain Mapp.*, 14(3):140–151.

- Calhoun, V. D., Liu, J., and Adalı, T. (2009). A review of group ICA for fMRI data and ICA for joint inference of imaging, genetic, and ERP data. *Neuroimage*, 45(1):S163–S172.
- Cao, K., Gong, Q., Hong, Y., and Wan, L. (2022). A unified computational framework for single-cell data integration with optimal transport. *Nat. Comm.*, 13(1).
- Cardoso, J. and Souselas, A. (1993). Blind beamforming for non-gaussian signals. *IEE Proceedings F Radar and Signal Processing*, 140(6):362.
- Chabriel, G., Kleinstüber, M., Moreau, E., Shen, H., Tichavsky, P., and Yeredor, A. (2014). Joint matrices decompositions and blind source separation: A survey of methods, identification, and applications. *IEEE Signal Process. Mag.*, 31(3):34–43.
- Chen, Z., Xie, F., Qiao, J., Hao, Z., Zhang, K., and Cai, R. (2022). Identification of linear latent variable model with arbitrary distribution. *Proceedings of the AAAI Conference on Artificial Intelligence*, 36(6):6350–6357.
- Comon, P. (1994). Independent component analysis, a new concept? *Signal Process.*, 36(3):287–314.
- Comon, P. and Jutten, C. (2010). *Handbook of Blind Source Separation: Independent Component Analysis and Applications*. Elsevier.
- Dai, H., Spirtes, P., and Zhang, K. (2022). Independence testing-based approach to causal discovery under measurement error and linear non-gaussian models. *arXiv preprint arXiv:2210.11021*.
- Duren, Z., Chen, X., Zamanighomi, M., Zeng, W., Satpathy, A. T., Chang, H. Y., Wang, Y., and Wong, W. H. (2018). Integrative analysis of single-cell genomics data by coupled nonnegative matrix factorizations. *Proc. Natl. Acad. Sci.*, 115(30):7723–7728.
- Ericsson, L., Gouk, H., Loy, C. C., and Hospedales, T. M. (2022). Self-supervised representation learning: Introduction, advances, and challenges. *IEEE Signal Process. Mag.*, 39(3):42–62.
- Eriksson, J. and Koivunen, V. (2004). Identifiability, separability, and uniqueness of linear ICA models. *IEEE Signal Process. Lett.*, 11(7):601–604.
- Esposito, F., Scarabino, T., Hyvärinen, A., Himberg, J., Formisano, E., Comani, S., Tedeschi, G., Goebel, R., Seifritz, E., and Di Salle, F. (2005). Independent component analysis of fMRI group studies by self-organizing clustering. *Neuroimage*, 25(1):193–205.
- Gentle, J. E. (1998). *Numerical linear algebra for applications in statistics*. Statistics and Computing. Springer-Verlag, New York.
- Gessel, I. and Viennot, G. (1985). Binomial determinants, paths, and hook length formulae. *Adv. in Math.*, 58(3):300–321.
- Gossi, F., Pati, P., Martinelli, A., and Rapsomaniki, M. A. (2022). MatchCLOT: Single-cell modality matching with contrastive learning and optimal transport. *bioRxiv preprint*.
- Gresele, L., Rubenstein, P. K., Mehrjou, A., Locatello, F., and Schölkopf, B. (2020). The incomplete rosetta stone problem: Identifiability results for multi-view nonlinear ICA. In Adams, R. P. and Gogate, V., editors, *Proceedings of The 35th Uncertainty in Artificial Intelligence Conference*, volume 115 of *Proceedings of Machine Learning Research*, pages 217–227. PMLR.
- Huang, B., Low, C. J. H., Xie, F., Glymour, C., and Zhang, K. (2022). Latent hierarchical causal structure discovery with rank constraints. *arXiv preprint*



*arXiv:2210.01798*.

- Hyvärinen, A. (1999). Fast and robust fixed-point algorithms for independent component analysis. *IEEE Trans. Neural Netw.*, 10(3):626–634.
- Hyvärinen, A. and Oja, E. (2000). Independent component analysis: algorithms and applications. *Neural Netw.*, 13(4):411–430.
- Hyvärinen, A. and Ramkumar, P. (2013). Testing independent component patterns by inter-subject or inter-session consistency. *Front. Hum. Neurosci.*, 7:94.
- Khemakhem, I., Kingma, D., Monti, R., and Hyvärinen, A. (2020). Variational autoencoders and nonlinear ICA: A unifying framework. In Chiappa, S. and Calandra, R., editors, *Proceedings of the Twenty Third International Conference on Artificial Intelligence and Statistics*, volume 108 of *Proceedings of Machine Learning Research*, pages 2207–2217. PMLR.
- Kim, T., Lee, I., and Lee, T.-W. (2006). Independent vector analysis: definition and algorithms. In *2006 Fortieth Asilomar Conference on Signals, Systems and Computers*, pages 1393–1396. IEEE.
- Klami, A., Virtanen, S., Leppäaho, E., and Kaski, S. (2014). Group factor analysis. *IEEE Trans. Neural Netw. Learn. Syst.*, 26(9):2136–2147.
- Li, X.-L., Adalı, T., and Anderson, M. (2011). Joint blind source separation by generalized joint diagonalization of cumulant matrices. *Signal Process.*, 91(10):2314–2322.
- Lin, Y., Wu, T.-Y., Wan, S., Yang, J. Y., Wong, W. H., and Wang, Y. (2022). scJoint integrates atlas-scale single-cell RNA-seq and ATAC-seq data with transfer learning. *Nat. Biotechnol.*, 40(5):703–710.
- Lindström, B. (1973). On the vector representations of induced matroids. *Bull. London Math. Soc.*, 5:85–90.
- Liu, J., Huang, Y., Singh, R., Vert, J.-P., and Noble, W. S. (2019). Jointly embedding multiple single-cell omics measurements. In Huber, K. T. and Gusfield, D., editors, *19th International Workshop on Algorithms in Bioinformatics (WABI 2019)*, volume 143 of *Leibniz International Proceedings in Informatics (LIPIcs)*, pages 10:1–10:13, Dagstuhl, Germany. Schloss Dagstuhl–Leibniz-Zentrum fuer Informatik.
- Liu, Y., Zhang, Z., Gong, D., Gong, M., Huang, B., Hengel, A. v. d., Zhang, K., and Shi, J. Q. (2022). Identifying weight-variant latent causal models. *arXiv preprint arXiv:2208.14153*.
- Lopez, R., Tagasovska, N., Ra, S., Cho, K., Pritchard, J., and Regev, A. (2022). Learning causal representations of single cells via sparse mechanism shift modeling. In *NeurIPS 2022 Workshop on Causality for Real-world Impact*.
- Lukic, A. S., Wernick, M. N., Hansen, L. K., and Strother, S. C. (2002). An ICA algorithm for analyzing multiple data sets. In *Proceedings. International Conference on Image Processing*, volume 2, pages II–II. IEEE.
- Lyche, T. (2020). *Numerical linear algebra and matrix factorizations*, volume 22 of *Texts in Computational Science and Engineering*. Springer, Cham. With a foreword by Geir Dahl.
- Maneshi, M., Vahdat, S., Gotman, J., and Grova, C. (2016). Validation of shared and specific independent component analysis (SSICA) for between-group comparisons in fMRI. *Front. Neurosci.*, 10:417.
- Mesters, G. and Zwiernik, P. (2022). Non-independent components analysis. *arXiv preprint arXiv:2206.13668*.

- Nielsen, A. A. (2002). Multiset canonical correlations analysis and multispectral, truly multitemporal remote sensing data. *IEEE Trans. Image Process.*, 11(3):293–305.
- Pandeva, T. and Forré, P. (2022). Multi-view independent component analysis with shared and individual sources. *arXiv preprint arXiv:2210.02083*.
- Richard, H., Ablin, P., Thirion, B., Gramfort, A., and Hyvärinen, A. (2021). Shared independent component analysis for multi-subject neuroimaging. *Adv. Neural Inf. Process. Syst.*, 34:29962–29971.
- Schölkopf, B., Locatello, F., Bauer, S., Ke, N. R., Kalchbrenner, N., Goyal, A., and Bengio, Y. (2021). Toward causal representation learning. *Proc. IEEE*, 109(5):612–634.
- Seigal, A., Squires, C., and Uhler, C. (2022). Linear causal disentanglement via interventions. *arXiv preprint arXiv:2211.16467*.
- Shimizu, S., Inazumi, T., Sogawa, Y., Hyvärinen, A., Kawahara, Y., Washio, T., Hoyer, P. O., and Bollen, K. (2011). DirectLiNGAM: a direct method for learning a linear non-Gaussian structural equation model. *J. Mach. Learn. Res.*, 12:1225–1248.
- Silva, R., Scheine, R., Glymour, C., and Spirtes, P. (2006). Learning the structure of linear latent variable models. *J. Mach. Learn. Res.*, 7(8):191–246.
- Stuart, T., Butler, A., Hoffman, P., Hafemeister, C., Papalexi, E., Mauck, W. M., Hao, Y., Stoekius, M., Smibert, P., and Satija, R. (2019). Comprehensive integration of single-cell data. *Cell*, 177(7):1888–1902.e21.
- Sui, J., Adali, T., Pearlson, G. D., and Calhoun, V. D. (2009). An ICA-based method for the identification of optimal fMRI features and components using combined group-discriminative techniques. *Neuroimage*, 46(1):73–86.
- Svensén, M., Kruggel, F., and Benali, H. (2002). ICA of fMRI group study data. *Neuroimage*, 16(3):551–563.
- van der Vaart, A. W. and Wellner, J. A. (1996). *Weak convergence and empirical processes*. Springer Series in Statistics. Springer-Verlag, New York. With applications to statistics.
- Varoquaux, G., Sadaghiani, S., Poline, J. B., and Thirion, B. (2009). CanICA: Model-based extraction of reproducible group-level ICA patterns from fMRI time series. In *Medical Image Computing and Computer Aided Intervention*, page 1.
- Wang, Y. S. and Drton, M. (2020). High-dimensional causal discovery under non-Gaussianity. *Biometrika*, 107(1):41–59.
- Welch, J. D., Hartemink, A. J., and Prins, J. F. (2017). MATCHER: manifold alignment reveals correspondence between single cell transcriptome and epigenome dynamics. *Genome Biol.*, 18(1):1–19.
- Xie, F., Cai, R., Huang, B., Glymour, C., Hao, Z., and Zhang, K. (2020). Generalized independent noise condition for estimating latent variable causal graphs. In Larochelle, H., Ranzato, M., Hadsell, R., Balcan, M., and Lin, H., editors, *Adv. in Neural Inf. Process. Syst.*, volume 33, pages 14891–14902. Curran Associates, Inc.
- Xie, F., Huang, B., Chen, Z., He, Y., Geng, Z., and Zhang, K. (2022). Identification of linear non-Gaussian latent hierarchical structure. In Chaudhuri, K., Jegelka, S., Song, L., Szepesvari, C., Niu, G., and Sabato, S., editors, *Proceedings of the 39th International Conference on Machine Learning*, volume 162 of *Proceedings of Machine Learning Research*, pages 24370–24387. PMLR.

- Yang, K. D., Belyaeva, A., Venkatachalapathy, S., Damodaran, K., Katcoff, A., Radhakrishnan, A., Shivashankar, G. V., and Uhler, C. (2021a). Multi-domain translation between single-cell imaging and sequencing data using autoencoders. *Nat. Comm.*, 12(1).
- Yang, K. D. and Uhler, C. (2019). Multi-domain translation by learning uncoupled autoencoders. *Computational Biology Workshop, International Conference on Machine Learning*.
- Yang, M., Liu, F., Chen, Z., Shen, X., Hao, J., and Wang, J. (2021b). Causalvae: Disentangled representation learning via neural structural causal models. In *Proceedings of the IEEE/CVF Conference on Computer Vision and Pattern Recognition (CVPR)*, pages 9593–9602.
- Yuan, Q. and Duren, Z. (2022). Integration of single-cell multi-omics data by regression analysis on unpaired observations. *Genome Biol.*, 23(1):1–19.
- Zhu, J.-Y., Park, T., Isola, P., and Efros, A. A. (2017). Unpaired image-to-image translation using cycle-consistent adversarial networks. In *2017 IEEE International Conference on Computer Vision (ICCV)*, pages 2242–2251.
- Zhuang, F., Qi, Z., Duan, K., Xi, D., Zhu, Y., Zhu, H., Xiong, H., and He, Q. (2021). A comprehensive survey on transfer learning. *Proc. IEEE*, 109(1):43–76.

## APPENDIX A. PROOFS

## A.1. Proofs of Section 3.

*Proof of Theorem 3.1.* Let  $P_X \in \mathcal{M}(\mathcal{G}_m)$  for an  $m$ -domain graph  $\mathcal{G}_m = (\mathcal{H} \cup V, D)$  with shared latent nodes  $\mathcal{L} = [\ell]$  and representation  $(B, P)$ . By Condition (C1) the measure  $P$  has independent, non-degenerate, non-symmetric marginals  $P_i$ ,  $i \in \mathcal{H}$  with mean zero and variance one. Moreover, since  $B \in \text{Im}(\phi_{\mathcal{G}_m})$ , we have  $B = G(I - A)^{-1}$  for matrices  $G \in \mathbb{R}^{D \times \mathcal{H}}$  and  $A \in \mathbb{R}^{D \times \mathcal{H}}$ .

Fix one domain  $e \in [m]$ . Recall that we denote by  $S_e = \text{pa}(V_e) = \mathcal{L} \cup I_e$  the set of latent parents in domain  $e$ . Define the matrix

$$B^e := G_{V_e, S_e} [(I - A)^{-1}]_{S_e, S_e} = G^e [(I - A)^{-1}]_{S_e, S_e},$$

and observe that we can write  $P_{X^e} = B_{V_e, \mathcal{H}} \# P = B^e \# P_{S_e}$ . This is due to the fact that  $G_{V_e, \mathcal{H} \setminus S_e} = 0$  and  $[(I - A)^{-1}]_{S_e, \mathcal{H} \setminus S_e} = 0$  by the definition of an  $m$ -domain graph.

In particular, the equality  $P_{X^e} = B^e \# P_{S_e}$  shows that the representation in Line 4 of Algorithm 1 exists. Now, we show that it is unique up to signed permutation by applying results on identifiability of linear ICA. Since  $G^e$  has full column rank by Condition (C2) and  $[(I - A)^{-1}]_{S_e, S_e}$  is invertible, the matrix  $B^e$  also has full column rank. Let  $P_{X^e} = \widehat{B}^e \# P^e$  be any representation, where  $\widehat{B}^e \in \mathbb{R}^{d_e \times s_e}$  and  $P^e$  is an  $\widehat{s}_e$ -dimensional probability measure with independent, non-degenerate marginals  $P_i^e$ . Due to Condition (C1), all probability measures  $P_i$  are non-Gaussian and non-degenerate and therefore we have by Eriksson and Koivunen (2004, Theorem 3 and 4) the identities

$$(4) \quad \widehat{B}^e = B^e R^e \Lambda^e \quad \text{and} \quad P^e = \Lambda^e (R^e)^\top \# P_{S_e},$$

where  $\Lambda^e$  is an  $s_e \times s_e$  diagonal matrix with nonzero entries and  $R^e$  is an  $s_e \times s_e$  permutation matrix. In particular, we have  $\widehat{s}_e = s_e$ , which means that  $\widehat{B}^e \in \mathbb{R}^{d_e \times s_e}$  and that  $P^e$  is an  $s_e$ -dimensional probability measure. Line 4 also requires that each marginal  $P_i^e$  has unit variance. This removes the scaling indeterminacy in (4) and we have

$$\widehat{B}^e = B^e R^e D^e \quad \text{and} \quad P^e = D^e (R^e)^\top \# P_{S_e},$$

where  $D^e$  is a diagonal matrix with entries  $D_{ii}^e \in \{\pm 1\}$ . In particular, this means that the distributions  $P^e$  and  $P_{S_e}$  coincide up to permutation and sign of the marginals.

The matching in Line 6 identifies which components of  $P^e$  are shared. By Condition (C1), two components of different domains  $P_i^e$  and  $P_j^f$  are shared if and only if they coincide up to sign, that is, if and only if  $d(P_i^e, P_j^f) = 0$  or  $d(P_i^e, -P_j^f) = 0$ . If their distribution coincide up to sign, then either  $d(P_i^e, P_j^f) = 0$  or  $d(P_i^e, -P_j^f) = 0$  but not both since Condition (C1) requires the distribution of the error variables to be non-symmetric. We conclude that in each domain  $e \in [m]$  there exists an  $s_e \times s_e$  signed permutation matrix  $Q^e$  such that

$$(5) \quad d([(Q^e)^\top \# P^e]_i, [(Q^f)^\top \# P^f]_i) = 0$$

for all  $i = 1, \dots, \widehat{\ell}$  and for all  $f \neq e$ . In particular,  $\widehat{\ell} = \ell$  and  $\widehat{\mathcal{L}} = \mathcal{L}$ .

It remains to show that  $\widehat{B} = B\Psi$  and  $\widehat{P} = \Psi^\top \# P$  for a signed permutation block matrix  $\Psi \in \Pi$ . By Equation (5), the distributions  $[(Q^e)^\top \# P^e]_{\mathcal{L}}$  and  $[(Q^e)^\top \# P^e]_{\mathcal{L}}$

coincide, which means that

$$(6) \quad (Q^e)^\top \# P^e = (Q^e)^\top D^e (R^e)^\top \# P_{S_e} = \begin{pmatrix} \Psi_{\mathcal{L}}^\top & 0 \\ 0 & \Psi_{I_e}^\top \end{pmatrix} \# \begin{pmatrix} P_{\mathcal{L}} \\ P_{I_e} \end{pmatrix},$$

where  $\Psi_{\mathcal{L}}$  is an  $\ell \times \ell$  signed permutation matrix and  $\Psi_{I_e}$  is an  $|I_e| \times |I_e|$  signed permutation matrix. Importantly, the matrix  $\Psi_{\mathcal{L}}^\top$  does not depend on the domain  $e \in [m]$ . Hence, the matrix  $\Phi^e := R^e D^e Q^e$  is a signed permutation matrix with block structure as in Equation (6). Moreover, we have

$$\widehat{B}^e Q^e = B^e R^e D^e Q^e = B^e \Phi^e = \left( B_{\mathcal{L}}^e \Psi_{\mathcal{L}} \mid B_{[s_e] \setminus \mathcal{L}}^e \Psi_{I_e} \right),$$

which means that the matrix  $\widehat{B}$  can be factorized as

$$\begin{aligned} \widehat{B} &= \begin{pmatrix} [\widehat{B}^1 Q^1]_{\widehat{\mathcal{L}}} & [\widehat{B}^1 Q^1]_{[s_1] \setminus \widehat{\mathcal{L}}} & & \\ \vdots & & \ddots & \\ [\widehat{B}^m Q^m]_{\widehat{\mathcal{L}}} & & & [\widehat{B}^m Q^m]_{[s_m] \setminus \widehat{\mathcal{L}}} \end{pmatrix} \\ &= \begin{pmatrix} B_{\mathcal{L}}^1 \Psi_{\mathcal{L}} & B_{[s_1] \setminus \mathcal{L}}^1 \Psi_{I_1} & & \\ \vdots & & \ddots & \\ B_{\mathcal{L}}^m \Psi_{\mathcal{L}} & & & B_{[s_m] \setminus \mathcal{L}}^m \Psi_{I_m} \end{pmatrix} \\ &= \begin{pmatrix} B_{\mathcal{L}}^1 & B_{[s_1] \setminus \mathcal{L}}^1 & & \\ \vdots & & \ddots & \\ B_{\mathcal{L}}^m & & & B_{[s_m] \setminus \mathcal{L}}^m \end{pmatrix} \cdot \begin{pmatrix} \Psi_{\mathcal{L}} & & & \\ & \Psi_{I_1} & & \\ & & \ddots & \\ & & & \Psi_{I_m} \end{pmatrix} = B \cdot \Psi, \end{aligned}$$

where  $\Psi \in \Pi$ . Similarly, we have for all  $e \in [m]$ ,

$$(Q^e)^\top \# P^e = (\Phi^e)^\top \# P_{S_e} = \begin{pmatrix} (\Psi_{\mathcal{L}})^\top \# P_{\mathcal{L}} \\ (\Psi_{I_e})^\top \# P_{I_e} \end{pmatrix}.$$

We conclude that

$$\begin{aligned} \widehat{P} &= \begin{pmatrix} [(Q^1)^\top \# P^1]_{\widehat{\mathcal{L}}} \\ [(Q^1)^\top \# P^1]_{[s_1] \setminus \widehat{\mathcal{L}}} \\ \vdots \\ [(Q^m)^\top \# P^m]_{[s_m] \setminus \widehat{\mathcal{L}}} \end{pmatrix} = \begin{pmatrix} (\Psi_{\mathcal{L}})^\top \# P_{\mathcal{L}} \\ (\Psi_{I_1})^\top \# P_{I_1} \\ \vdots \\ (\Psi_{I_m})^\top \# P_{I_m} \end{pmatrix} \\ &= \begin{pmatrix} \Psi_{\mathcal{L}} & & & \\ & \Psi_{I_1} & & \\ & & \ddots & \\ & & & \Psi_{I_m} \end{pmatrix}^\top \# \begin{pmatrix} P_{\mathcal{L}} \\ P_{I_1} \\ \vdots \\ P_{I_m} \end{pmatrix} = \Psi^\top \# P. \end{aligned}$$

□

*Proof of Theorem 3.5.* Let  $C = (i_1, \dots, i_m)$  and  $g$  be as in the statement of the theorem. W.l.o.g. we assume that  $E = \{1, \dots, |E|\}$  and that  $T(\widehat{P}_{i_e}^e, \widehat{P}_{i_f}^f) \leq T(\widehat{P}_{i_e}^e, -\widehat{P}_{i_f}^f)$ . Observe that  $C$  determines a shared node if and only if

$$\sum_{e < f} \Omega_\alpha(\widehat{P}_{i_e}^e, \widehat{P}_{i_f}^f) = \binom{m}{2}.$$

Now, we have

$$\begin{aligned}
& P\left(\sum_{e<f} \Omega_\alpha(\widehat{P}_{i_e}^e, \widehat{P}_{i_f}^f) = \binom{m}{2}\right) \\
&= P\left(\bigcap_{e<f} \{\Omega_\alpha(\widehat{P}_{i_e}^e, \widehat{P}_{i_f}^f) = 1\}\right) \\
&\leq P\left(\bigcap_{e<f} \{T_{ij}^{ef} \leq c_\alpha\}\right) \\
&= P\left(\bigcap_{e<f} \{T(\widehat{P}_{i_e}^e, \widehat{P}_{i_f}^f) \leq c_\alpha\} \cup \{T(\widehat{P}_{i_e}^e, -\widehat{P}_{i_f}^f) \leq c_\alpha\}\right) \\
&\leq P\left(\bigcap_{e<f} \{T(\widehat{P}_{i_e}^e, \widehat{P}_{i_f}^f) \leq c_\alpha\}\right) \\
(7) \quad &\leq P\left(\bigcap_{\substack{e \in E, f \in [m] \\ e < f}} \{T(\widehat{P}_{i_e}^e, \widehat{P}_{i_f}^f) \leq c_\alpha\}\right).
\end{aligned}$$

By the triangle inequality we have

$$(8) \quad d_{\text{KS}}(P_{i_e}^e, P_{i_f}^f) \leq d_{\text{KS}}(P_{i_e}^e, \widehat{P}_{i_e}^e) + d_{\text{KS}}(\widehat{P}_{i_e}^e, \widehat{P}_{i_f}^f) + d_{\text{KS}}(\widehat{P}_{i_f}^f, P_{i_f}^f).$$

Moreover, if  $e \in E$  and  $f \in [m]$ , then we have by Condition (ii)

$$(9) \quad d_{\text{KS}}(P_{i_e}^e, P_{i_f}^f) \geq \kappa.$$

Using (8) and (9) together with the fact  $\sqrt{\frac{n_e n_f}{n_e + n_f}} \geq \frac{n_{\min}}{\sqrt{2n_{\max}}}$ , we obtain the following chain of implications for  $e \in E$  and  $f \in [m]$ :

$$\begin{aligned}
& T(\widehat{P}_{i_e}^e, \widehat{P}_{i_f}^f) \leq c_\alpha \\
&\iff \sqrt{\frac{n_e n_f}{n_e + n_f}} d_{\text{KS}}(\widehat{P}_{i_e}^e, \widehat{P}_{i_f}^f) \leq c_\alpha \\
&\implies \frac{n_{\min}}{\sqrt{2n_{\max}}} \left( d_{\text{KS}}(P_{i_e}^e, P_{i_f}^f) - d_{\text{KS}}(\widehat{P}_{i_e}^e, P_{i_e}^e) - d_{\text{KS}}(\widehat{P}_{i_f}^f, P_{i_f}^f) \right) \leq c_\alpha \\
&\implies \frac{n_{\min}}{\sqrt{2n_{\max}}} \left( \kappa - d_{\text{KS}}(\widehat{P}_{i_e}^e, P_{i_e}^e) - d_{\text{KS}}(\widehat{P}_{i_f}^f, P_{i_f}^f) \right) \leq c_\alpha \\
&\iff d_{\text{KS}}(\widehat{P}_{i_e}^e, P_{i_e}^e) + d_{\text{KS}}(\widehat{P}_{i_f}^f, P_{i_f}^f) \geq \kappa - \frac{\sqrt{2n_{\max}}}{n_{\min}} c_\alpha \\
&\implies \left\{ d_{\text{KS}}(\widehat{P}_{i_e}^e, P_{i_e}^e) \geq \frac{\kappa}{2} - \frac{\sqrt{n_{\max}}}{\sqrt{2} n_{\min}} c_\alpha \right\} \text{ or } \left\{ d_{\text{KS}}(\widehat{P}_{i_f}^f, P_{i_f}^f) \geq \frac{\kappa}{2} - \frac{\sqrt{n_{\max}}}{\sqrt{2} n_{\min}} c_\alpha \right\}.
\end{aligned}$$

Now, consider the event  $\bigcap_{\substack{e \in E, f \in [m] \\ e < f}} \{T(\widehat{P}_{i_e}^e, \widehat{P}_{i_f}^f) \leq c_\alpha\}$ . On this event, there cannot be two elements  $e, e^* \in E$  such that both

$$\left\{ d_{\text{KS}}(\widehat{P}_{i_e}^e, P_{i_e}^e) < \frac{\kappa}{2} - \frac{\sqrt{n_{\max}}}{\sqrt{2} n_{\min}} c_\alpha \right\} \text{ and } \left\{ d_{\text{KS}}(\widehat{P}_{i_{e^*}}^{e^*}, P_{i_{e^*}}^{e^*}) < \frac{\kappa}{2} - \frac{\sqrt{n_{\max}}}{\sqrt{2} n_{\min}} c_\alpha \right\}.$$

To see this recall that  $E \subseteq [m]$ . We conclude that it must hold  $\{d_{\text{KS}}(\widehat{P}_{i_e}^e, P_{i_e}^e) \geq \frac{\kappa}{2} - \frac{\sqrt{n_{\max}}}{\sqrt{2} n_{\min}} c_\alpha\}$  for all but at most one element of  $E$ . We denote this exceptional element by  $e^* \in E$ . Taking up (7), we get the following:

$$\begin{aligned}
& P\left(\sum_{e < f} \Omega_\alpha(\widehat{P}_{i_e}^e, \widehat{P}_{i_f}^f) = \binom{m}{2}\right) \\
& \leq P\left(\bigcap_{\substack{e \in E, f \in [m] \\ e < f}} \{T(\widehat{P}_{i_e}^e, \widehat{P}_{i_f}^f) \leq c_\alpha\}\right) \\
& \leq P\left(\bigcap_{e \in E \setminus \{e^*\}} \left\{d_{\text{KS}}(\widehat{P}_{i_e}^e, P_{i_e}^e) \geq \frac{\kappa}{2} - \frac{\sqrt{n_{\max}}}{\sqrt{2} n_{\min}} c_\alpha\right\}\right) \\
(10) \quad & = \prod_{e \in E \setminus \{e^*\}} P\left(d_{\text{KS}}(\widehat{P}_{i_e}^e, P_{i_e}^e) \geq \frac{\kappa}{2} - \frac{\sqrt{n_{\max}}}{\sqrt{2} n_{\min}} c_\alpha\right) \\
(11) \quad & = \prod_{e \in E \setminus \{e^*\}} P\left(d_{\text{KS}}(\widehat{P}_{i_e}^e, P_{i_e}^e) \geq \max\left\{\frac{\kappa}{2} - \frac{\sqrt{n_{\max}}}{\sqrt{2} n_{\min}} c_\alpha, 0\right\}\right) \\
(12) \quad & \leq g\left(n_{\min}, \max\left\{\frac{\kappa}{2} - \frac{\sqrt{n_{\max}}}{\sqrt{2} n_{\min}} c_\alpha, 0\right\}\right)^{|E|-1}.
\end{aligned}$$

The last three steps need more explanation: Equality (10) follows from the fact that domains are unpaired. That is, the distances  $d_{\text{KS}}(\widehat{P}_{i_e}^e, P_{i_e}^e)$  and  $d_{\text{KS}}(\widehat{P}_{i_f}^f, P_{i_f}^f)$  are pairwise independent for different domains  $e, f \in [m]$ . Equality (11) is trivial since  $d_{\text{KS}}(\widehat{P}_{i_e}^e, P_{i_e}^e) \geq 0$ . Finally, Inequality (12) follows from Condition (i) and that the function  $g$  is monotonically decreasing in  $n$ . We also used the fact that  $|E \setminus \{e^*\}| = |E| - 1$ .  $\square$

## A.2. Proofs of Section 4.

Before proving Lemma 4.3 and Theorem 4.4 we fix some notation. Let  $\mathcal{G}_m = (V \cup \mathcal{H}, D)$  be an  $m$ -domain graph. We denote by  $\text{anc}(v) = \{k \in \mathcal{H} : \text{there is a directed path } k \rightarrow \dots \rightarrow v \text{ in } \mathcal{G}_m\}$  the ancestors of a node  $v \in V$ . For subsets  $W \subseteq V$ , we denote  $\text{anc}(W) = \bigcup_{v \in W} \text{anc}(v)$ . Moreover, for  $\mathcal{L} \subseteq \mathcal{H}$  and  $v \in V$ , we write shortly  $\text{pa}_{\mathcal{L}}(v) = \text{pa}(v) \cap \mathcal{L}$ .

*Proof of Lemma 4.3.* Let  $B \in \text{Im}(\phi_{\mathcal{G}_m})$ . Then we can write  $B = G \cdot (I - A)^{-1}$  with

$$G = \left( \begin{array}{c|ccc} G_{V_1, \mathcal{L}} & G_{V_1, I_1} & & \\ \vdots & & \ddots & \\ G_{V_m, \mathcal{L}} & & & G_{V_m, I_m} \end{array} \right).$$

Moreover, observe that, by the definition of an  $m$ -domain-graph, the matrix  $B_{V, \mathcal{L}}$  factorizes as

$$B_{V, \mathcal{L}} = G_{V, \mathcal{L}}[(I - A)^{-1}]_{\mathcal{L}, \mathcal{L}}.$$

Now, suppose that  $i$  and  $j$  are partial pure children of a fixed node  $k \in \mathcal{L}$ . Then  $\text{pa}_{\mathcal{L}}(i) = \{k\} = \text{pa}_{\mathcal{L}}(j)$ . In particular, the only entry that may be nonzero in the

row  $G_{i,\mathcal{L}}$  is given by  $G_{ik}$  and the only entry that may be nonzero in the row  $G_{j,\mathcal{L}}$  is given by  $G_{jk}$ . Thus, we have

$$B_{i,\mathcal{L}} = \sum_{q \in \mathcal{L}} G_{iq}[(I - A)^{-1}]_{q,\mathcal{L}} = G_{ik}[(I - A)^{-1}]_{k,\mathcal{L}}.$$

Similarly, it follows that  $B_{j,\mathcal{L}} = G_{jk}[(I - A)^{-1}]_{k,\mathcal{L}}$ . This means that the row  $B_{j,\mathcal{L}}$  is a multiple of the row  $B_{i,\mathcal{L}}$  and we conclude that  $\text{rank}(B_{\{i,j\},\mathcal{L}}) \leq 1$ . Equality holds due to the faithfulness condition (C4) which implies that  $B_{ik} \neq 0$  and  $B_{jk} \neq 0$ , i.e.,  $B_{\{i,j\},\mathcal{L}}$  is not the null matrix.

For the other direction suppose that  $\text{rank}(B_{\{i,j\},\mathcal{L}}) = 1$ . By applying the Lindström-Gessel-Viennot Lemma (Gessel and Viennot, 1985; Lindström, 1973) equivalently as in Dai et al. (2022, Theorem 1 and 2), it can be seen that

$$(13) \quad \text{rank}(B_{\{i,j\},\mathcal{L}}) \leq \min \{ |S| : S \text{ is a vertex cut from } \text{anc}(\mathcal{L}) \text{ to } \{i, j\} \},$$

where  $S$  is a vertex cut from  $\text{anc}(\mathcal{L})$  to  $\{i, j\}$  if and only if there exists no directed path in  $\mathcal{G}_m$  from  $\text{anc}(\mathcal{L})$  to  $\{i, j\}$  without passing through  $S$ . Moreover, equality holds in (13) for generic (almost all) choices of parameters. Since we assumed rank faithfulness in Condition (C4) we exclude cases where the inequality is strict and therefore have equality. By the definition of an  $m$ -domain graph we have that  $\text{anc}(\mathcal{L}) = \mathcal{L}$ . Thus, if  $\text{rank}(B_{\{i,j\},\mathcal{L}}) = 1$ , there must be a single node  $k \in \mathcal{L}$  such that  $\{k\}$  is a vertex cut from  $\mathcal{L}$  to  $\{i, j\}$ . But then it follows that  $i$  and  $j$  have to be partial pure children of  $k$  by the definition of an  $m$ -domain graph and by using the assumption that there are no zero-rows in  $B_{\mathcal{L}}$ .  $\square$

To prove Theorem 2 we need the following auxiliary lemma.

**Lemma A.1.** *Let  $G = (V, D)$  be a DAG with topologically ordered nodes  $V = [p]$  and let  $M$  be a lower triangular matrix with entries  $M_{ii} \neq 0$  for all  $i = 1, \dots, p$  and  $M_{ij} \neq 0$  if and only if there is a directed path  $j \rightarrow \dots \rightarrow i$  in  $G$ . Let  $Q_{\sigma_1}$  and  $Q_{\sigma_2}$  be permutation matrices. Then the matrix  $Q_{\sigma_1} M Q_{\sigma_2}$  is lower triangular if and only if  $\sigma_2 = \sigma_1^{-1}$  and  $\sigma_2 \in \mathcal{S}(G)$ .*

*Proof of Lemma A.1.* By the definition of a permutation matrix, we have

$$(14) \quad [Q_{\sigma_1} M Q_{\sigma_2}]_{ij} = M_{\sigma_1(i)\sigma_2^{-1}(j)} \quad \text{or, equivalently,} \quad [Q_{\sigma_1} M Q_{\sigma_2}]_{\sigma_1^{-1}(i)\sigma_2(j)} = M_{ij}.$$

First, suppose that  $\sigma_2 = \sigma_1^{-1}$  and  $\sigma_2 \in \mathcal{S}(G)$ , and let  $i, j \in [p]$  such that  $\sigma_2(i) < \sigma_2(j)$ . Then, by the definition of  $\mathcal{S}(G)$ , there is no directed path  $j \rightarrow \dots \rightarrow i$  in the graph  $G$  and therefore we have  $M_{ij} = 0$ . But this means that  $[Q_{\sigma_1} M Q_{\sigma_2}]_{\sigma_2(i)\sigma_2(j)} = 0$  and we conclude that the matrix  $Q_{\sigma_1} M Q_{\sigma_2}$  is lower triangular.

Now, assume that  $Q_{\sigma_1} M Q_{\sigma_2}$  is lower triangular, where  $\sigma_1$  and  $\sigma_2$  are arbitrary permutations on the set  $[p]$ . Since  $M$  has no zeros on the diagonal, we have  $M_{ii} = [Q_{\sigma_1} M Q_{\sigma_2}]_{\sigma_1^{-1}(i)\sigma_2(i)} \neq 0$  for all  $i = 1, \dots, p$ . It follows that  $\sigma_1^{-1}(i) \geq \sigma_2(i)$  for all  $i = 1, \dots, p$  because  $Q_{\sigma_1} M Q_{\sigma_2}$  is lower triangular. But this is only possible if the permutations coincide on all elements, i.e., we have  $\sigma_2 = \sigma_1^{-1}$ . It remains to show that  $\sigma_2 = \sigma_1^{-1} \in \mathcal{S}(G)$ . For any edge  $j \rightarrow i \in D$  we have that  $M_{ij} \neq 0$ . Recalling Equation (14) this means that  $[Q_{\sigma_1} M Q_{\sigma_2}]_{\sigma_2(i)\sigma_2(j)} \neq 0$ . But since  $Q_{\sigma_1} M Q_{\sigma_2}$  is lower triangular this can only be the case if  $\sigma_2(j) < \sigma_2(i)$  which proves that  $\sigma_2 \in \mathcal{S}(G)$ .  $\square$

*Proof of Theorem 4.4.* Each latent node in  $\mathcal{L}$  has two partial pure children by Condition (C3). After removing zero-rows in Line 3 of Algorithm 2 it holds by



Lemma 4.3 that  $\text{rank}(B_{\{i,j\},\mathcal{L}}^*) = 1$  if and only if there is a latent node in  $\mathcal{L}$  such that  $i$  and  $j$  are both partial pure children of that latent node. Hence, each tuple  $(i_k, j_k)_{k \in \mathcal{L}}$  in Line 4 of Algorithm 2 consists of two partial pure children of a certain latent node. The requirement  $\text{rank}(B_{\{i_k, i_q\}, \mathcal{L}}^*) = 2$  ensures that each pair of partial pure children has a different parent.

By the definition of an  $m$ -domain-graph and the fact that  $B^* = \widehat{B}_{\mathcal{L}}$ , for  $I = \{i_1, \dots, i_\ell\}$ , we have the factorization

$$(15) \quad B_{I,\mathcal{L}}^* = B_{I,\mathcal{L}} \Psi_{\mathcal{L}} = G_{I,\mathcal{L}} (I - A)_{\mathcal{L},\mathcal{L}}^{-1} \Psi_{\mathcal{L}} = G_{I,\mathcal{L}} (I - A_{\mathcal{L},\mathcal{L}})^{-1} \Psi_{\mathcal{L}},$$

where  $G \in \mathbb{R}^{D_V \times \mathcal{H}}$ ,  $A \in \mathbb{R}^{D_{\mathcal{H}} \times \mathcal{H}}$  and  $\Psi_{\mathcal{L}}$  is a signed permutation matrix. Let  $Q_1$  and  $Q_2$  be permutation matrices and let  $\Lambda$  be a diagonal matrix with non-zero diagonal elements and let  $D$  be a diagonal matrix with entries in  $\{\pm 1\}$ . Then we can rewrite Equation (15) as

$$B_{I,\mathcal{L}}^* = Q_1 \underbrace{\Lambda (I - A_{\mathcal{L},\mathcal{L}})^{-1} D}_{=: M} Q_2.$$

Now, we apply Lemma A.1. Since we assume throughout Section 4 that the nodes  $\mathcal{L}$  are topologically ordered, the matrix  $M$  is lower triangular with no zeros on the diagonal. Moreover, by Condition (C4) we have  $M_{ij} \neq 0$  if and only if there is a directed path  $j \rightarrow \dots \rightarrow i$  in  $\mathcal{G}_{\mathcal{L}}$ . In Line 6 we find other permutation matrices  $R_1$  and  $R_2$  such that

$$W = R_1 B_{I,\mathcal{L}}^* R_2 = (R_1 Q_1) M (Q_2 R_2)$$

is lower triangular. Now, define the permutation matrices  $Q_{\sigma_1} = R_1 Q_1$  and  $Q_{\sigma_2} = Q_2 R_2$ . Then we have by Lemma A.1 that  $Q_{\sigma_1} = Q_{\sigma_2}^\top$  and that  $\sigma_2 \in \mathcal{S}(\mathcal{G}_{\mathcal{L}})$ . Hence, the matrix  $W$  factorizes as

$$W = Q_{\sigma_2}^\top M Q_{\sigma_2} = Q_{\sigma_2}^\top \Lambda (I - A_{\mathcal{L},\mathcal{L}})^{-1} D Q_{\sigma_2} = \widetilde{\Lambda} Q_{\sigma_2}^\top (I - A_{\mathcal{L},\mathcal{L}})^{-1} Q_{\sigma_2} \widetilde{D},$$

where  $\widetilde{\Lambda}$  and  $\widetilde{D}$  are diagonal matrices with the entries given by permutations of the entries of  $\Lambda$  and  $D$ . Lines 7 and 8 address the scaling and sign matrices  $\widetilde{\Lambda}$  and  $\widetilde{D}$ . In particular, we have that  $\widetilde{W}' = D' Q_{\sigma_2}^\top (I - A_{\mathcal{L},\mathcal{L}})^{-1} Q_{\sigma_2} D'$  for another diagonal matrix  $D'$  with entries in  $\{\pm 1\}$ , since each entry on the diagonal of  $\widetilde{W}'$  is equal to 1. Thus, we have

$$\begin{aligned} \widehat{A} &= I - (\widetilde{W}')^{-1} \\ &= I - (D' Q_{\sigma_2}^\top (I - A_{\mathcal{L},\mathcal{L}})^{-1} Q_{\sigma_2} D')^{-1} \\ &= I - D' Q_{\sigma_2}^\top (I - A_{\mathcal{L},\mathcal{L}}) Q_{\sigma_2} D' \\ &= D' Q_{\sigma_2}^\top A_{\mathcal{L},\mathcal{L}} Q_{\sigma_2} D'. \end{aligned}$$

Since  $Q_{\sigma_2} D'$  is a signed permutation matrix with  $\sigma_2 \in \mathcal{S}(\mathcal{G}_{\mathcal{L}})$ , the first part of the theorem is proved. If  $G_{vk} > 0$  whenever  $v$  is a pure child of  $k$ , the matrix  $\widetilde{\Lambda}$  only has positive entries which means that  $D'$  is equal to the identity matrix. This proves the second part.  $\square$

## APPENDIX B. ADDITIONAL EXAMPLES

The graph in Figure 4 is an  $m$ -domain graph corresponding to the compact version in Figure 2 in the main paper.

**Example B.1.** Consider the  $m$ -domain graph in Figure 4. The linear structural equation model among the latent variables is determined by lower triangular matrices of the form

$$A = \begin{pmatrix} 0 & 0 & 0 & 0 & 0 \\ a_{21} & 0 & 0 & 0 & 0 \\ 0 & 0 & 0 & 0 & 0 \\ 0 & 0 & a_{43} & 0 & 0 \\ 0 & 0 & 0 & 0 & 0 \end{pmatrix}.$$

Moreover, the domain-specific mixing matrices  $G^e$  are of the form

$$G^1 = \begin{pmatrix} g_{11}^1 & g_{12}^1 & g_{13}^1 & 0 \\ g_{21}^1 & 0 & g_{23}^1 & 0 \\ 0 & g_{32}^1 & g_{33}^1 & g_{34}^1 \\ g_{41}^1 & g_{42}^1 & g_{43}^1 & g_{44}^1 \end{pmatrix} \quad \text{and} \quad G^2 = \begin{pmatrix} g_{11}^2 & 0 & g_{13}^2 \\ g_{21}^2 & g_{22}^2 & g_{23}^2 \\ 0 & g_{32}^2 & 0 \\ g_{41}^2 & g_{42}^2 & g_{43}^2 \\ g_{51}^2 & g_{52}^2 & 0 \end{pmatrix}.$$

Since the shared latent nodes are given by  $\mathcal{L} = \{1, 2\}$ , we have

$$G = \begin{pmatrix} g_{11}^1 & g_{12}^1 & g_{13}^1 & 0 & 0 \\ g_{21}^1 & 0 & g_{23}^1 & 0 & 0 \\ 0 & g_{32}^1 & g_{33}^1 & g_{34}^1 & 0 \\ g_{41}^1 & g_{42}^1 & g_{43}^1 & g_{44}^1 & 0 \\ g_{11}^2 & 0 & 0 & 0 & g_{13}^2 \\ g_{21}^2 & g_{22}^2 & 0 & 0 & g_{23}^2 \\ 0 & g_{32}^2 & 0 & 0 & 0 \\ g_{41}^2 & g_{42}^2 & 0 & 0 & g_{43}^2 \\ g_{51}^2 & g_{52}^2 & 0 & 0 & 0 \end{pmatrix}$$

and

$$B = G \cdot (I - A)^{-1} = \begin{pmatrix} a_{21}g_{12}^1 + g_{11}^1 & g_{12}^1 & g_{13}^1 & 0 & 0 \\ g_{21}^1 & 0 & g_{23}^1 & 0 & 0 \\ a_{21}g_{32}^1 & g_{32}^1 & a_{43}g_{34}^1 + g_{33}^1 & g_{34}^1 & 0 \\ a_{21}g_{42}^1 + g_{41}^1 & g_{42}^1 & a_{43}g_{44}^1 + g_{43}^1 & g_{44}^1 & 0 \\ g_{11}^2 & 0 & 0 & 0 & g_{13}^2 \\ a_{21}g_{22}^2 + g_{21}^2 & g_{22}^2 & 0 & 0 & g_{23}^2 \\ a_{21}g_{32}^2 & g_{32}^2 & 0 & 0 & 0 \\ a_{21}g_{42}^2 + g_{41}^2 & g_{42}^2 & 0 & 0 & g_{43}^2 \\ a_{21}g_{52}^2 + g_{51}^2 & g_{52}^2 & 0 & 0 & 0 \end{pmatrix}.$$

**Example B.2.** Consider the  $m$ -domain graph in Figure 4. The partial pure children of node  $1 \in \mathcal{L}$  are given by  $\{v_2^1, v_1^2\}$  and the partial pure children of  $2 \in \mathcal{L}$  are given by  $\{v_3^1, v_3^2\}$ . Moreover, by continuing Example B.1, we have that the matrix  $B_{\mathcal{L}}$  is

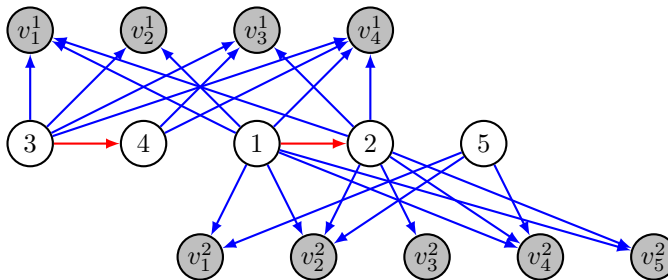


FIGURE 4. A 2-domain graph with 5 latent nodes and dimensions of the observed domains given by  $|V_1| = d_1 = 4$  and  $|V_2| = d_2 = 5$ . We denote  $V_e = \{v_1^e, \dots, v_{d_e}^e\}$ , that is, the superscript indicates the domain a node belongs to.

given by

$$B_{\mathcal{L}} = \begin{pmatrix} a_{21}g_{12}^1 + g_{11}^1 & g_{12}^1 \\ g_{21}^1 & 0 \\ a_{21}g_{32}^1 & g_{32}^1 \\ a_{21}g_{42}^1 + g_{41}^1 & g_{42}^1 \\ g_{11}^2 & 0 \\ a_{21}g_{22}^2 + g_{21}^2 & g_{22}^2 \\ a_{21}g_{32}^2 & g_{32}^2 \\ a_{21}g_{42}^2 + g_{41}^2 & g_{42}^2 \\ a_{21}g_{52}^2 + g_{51}^2 & g_{52}^2 \end{pmatrix}$$

It is easy to see that the two submatrices

$$\begin{pmatrix} g_{21}^1 & 0 \\ g_{11}^2 & 0 \end{pmatrix} \quad \text{and} \quad \begin{pmatrix} a_{21}g_{32}^1 & g_{32}^1 \\ a_{21}g_{32}^2 & g_{32}^2 \end{pmatrix}$$

have rank one. The first matrix corresponds to the partial pure children  $\{v_2^1, v_1^2\}$  in the graph in Figure 4 while the second matrix correspond to the partial pure children  $\{v_3^1, v_3^2\}$ . Note that the rank of any other  $2 \times 2$  submatrix is generically (i.e., almost surely) equal to 2.

### APPENDIX C. GAUSSIAN ERRORS

Without additional assumptions to those in Section 3, it is impossible to recover the joint distribution if the distributions of the errors  $\varepsilon_i$  of the latent structural equation model in Equation (1) are Gaussian. In this case, the distribution of  $Z$  as well as the distribution of each observed random vector  $X^e$  is determined by the covariance matrix only. The observed covariance matrix in domain  $e \in [m]$  is given by  $\Sigma^e = G^e \text{Cov}[Z_{\mathcal{L} \cup I_e}] (G^e)^\top$ . However, knowing  $\Sigma^e$  gives no information about  $Z_{\mathcal{L} \cup I_e}$  other than  $\text{rank}(\Sigma^e) = |\mathcal{L}| + |I_e|$ , that is, we cannot distinguish which latent variables are shared and which ones are domain-specific. This is formalized in the following lemma.

**Lemma C.1.** *Let  $\Sigma$  be any  $d \times d$  symmetric positive semidefinite matrix of rank  $p$  and let  $\Xi$  be another arbitrary  $p \times p$  symmetric positive definite matrix. Then there is  $G \in \mathbb{R}^{d \times p}$  such that  $\Sigma = G \Xi G^\top$ .*

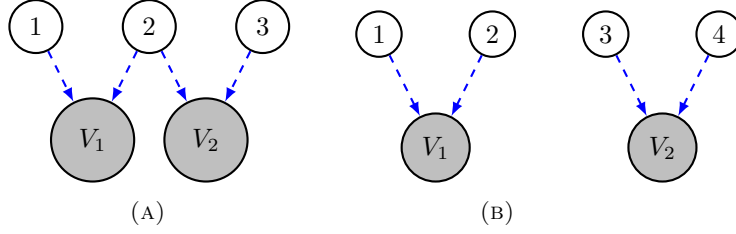


FIGURE 5. Compact versions of two 2-domain graphs. In both graphs, both domains have two latent parents. In setup (a) there is a shared latent parent while in setup (b) there is not.

*Proof.* Let  $\Sigma$  be a  $d \times d$  symmetric positive semidefinite matrix of rank  $p$ .  $\Sigma$  has a decomposition similar to the Cholesky decomposition; see e.g. Gentle (1998, Section 3.2.2). That is, there exists a unique matrix  $T$ , such that  $A = TT^\top$ , where  $T$  is a lower triangular matrix with  $p$  positive diagonal elements and  $d - p$  columns containing all zeros. Define  $\tilde{T}$  to be the  $d \times p$  matrix containing only the non-zero columns of  $T$ .

On the other hand, let  $\Xi$  be a symmetric positive definite  $p \times p$  matrix. By the usual Cholesky decomposition (Lyche, 2020, Section 4.2.1), there exists a unique  $p \times p$  lower triangular matrix  $L$  with positive diagonal elements such that  $\Xi = LL^\top$ . Now, define  $G := \tilde{T}L^{-1} \in \mathbb{R}^{d \times p}$ . Then,

$$\Sigma = \tilde{T}\tilde{T}^\top = \tilde{T}L^{-1}LL^\top L^{-\top}\tilde{T}^\top = G\xi G^\top. \quad \square$$

Due to Lemma C.1 it is necessary to consider non-Gaussian distributions to obtain identifiability of the joint distribution.

**Example C.2.** In the Gaussian case we cannot distinguish whether the two observed domains in Figure 5 share a latent variable or not. Said differently, the observed marginal distributions may either be generated by the mechanism defined by graph (a) or graph (b) and there is no way to distinguish from observational distributions only.

#### APPENDIX D. ALGORITHMS FOR FINITE SAMPLES

Algorithm 3 is the finite sample version of Algorithm 1 with the matching  $\Omega_\alpha$  defined in Definition 3.3. To determine the number of independent components for the linear ICA step in each domain, we need to check the  $\text{rank}(\mathbf{X}^e(\mathbf{X}^e)^\top)$ . We specify the rank of a matrix  $M$  as number of singular values which are larger than a certain threshold  $\gamma$  and denote it by  $\text{rank}_\gamma(M)$ . In Algorithm 4 we also provide a finite sample version of Algorithm 2 where we only have the approximation  $B^* = \hat{B}_\mathcal{L} \approx B_\mathcal{L}\Psi_\mathcal{L}$  for a signed permutation matrix  $\Psi_\mathcal{L}$ . For a matrix  $M$ , we denote by  $\sigma_{\min}(M)$  the smallest singular value.

#### APPENDIX E. ERROR DISTRIBUTIONS IN SIMULATIONS

We specify  $\mathcal{L} = \{1, 2, 3\}$ ,  $I_1 = \{4, 5\}$ ,  $I_2 = \{6, 7\}$  and  $I_3 = \{8, 9\}$ . Note that the set  $I_3$  does not exist if the number of domains is  $m = 2$ . The error distributions in all our simulations are specified as follows.

**Algorithm 3** IdentifyJointDistributionEmpirical

- 1: **Hyperparameters:**  $\gamma > 0$ ,  $\alpha \in (0, 1)$ .
- 2: **Input:** Matrix of observations  $\mathbf{X}^e \in \mathbb{R}^{d_e \times n_e}$  for all  $e \in [m]$ .
- 3: **Output:** Number of shared latent variables  $\hat{\ell}$ , matrix  $\hat{B}$  and probability measure  $\hat{P}$ .
- 4: **for**  $e \in [m]$  **do**
- 5: Linear ICA: Use any linear ICA algorithm to obtain a mixing matrix  $\tilde{B}^e \in \mathbb{R}^{d_e \times \hat{s}_e}$ , where  $\hat{s}_e = \text{rank}_\gamma(\mathbf{X}^e(\mathbf{X}^e)^\top)$ . Compute the matrix  $\tilde{\eta}^e = (\tilde{B}^e)^\dagger \mathbf{X}^e \in \mathbb{R}^{\hat{s}_e \times n_e}$ , where  $(\tilde{B}^e)^\dagger$  is the Moore-Penrose pseudoinverse of  $\tilde{B}^e$ .
- 6: Scaling: Let  $\Delta^e$  be a  $\hat{s}_e \times \hat{s}_e$  diagonal matrix with entries  $\Delta_{ii}^e = \frac{1}{n_e} [\tilde{\eta}^e (\tilde{\eta}^e)^\top]_{ii}$ . Define  $\hat{B}^e = \tilde{B}^e (\Delta^e)^{-1/2}$  and  $\eta^e = (\Delta^e)^{-1/2} \tilde{\eta}^e$ .
- 7: Let  $\hat{P}^e$  be the estimated probability measure with independent marginals such that  $\hat{P}_i^e$  is the empirical measure of the row  $\eta_{i,*}^e$ .
- 8: **end for**
- 9: Matching: Let  $\hat{\ell}$  be the maximal number such that there is a signed permutation matrix  $Q^e$  in each domain  $e \in [m]$  such that

$$\Omega_{\alpha_t}([(Q^e)^\top \# \hat{P}^e]_i, [(Q^f)^\top \# \hat{P}^f]_i) = 1$$

for all  $i = 1, \dots, \hat{\ell}$  and for all  $f \neq e$ , where  $\alpha_t = \alpha/t$  with  $t = 2 \sum_{e < f} \hat{s}_e \hat{s}_f$ .

- 10: Let  $\hat{\mathcal{L}} = \{1, \dots, \hat{\ell}\}$ .
- 11: Construct the matrix  $\hat{B}$  equal to

$$\left( \begin{array}{c|ccc} [\hat{B}^1 Q^1]_{\hat{\mathcal{L}}} & [\hat{B}^1 Q^1]_{[\hat{s}_1] \setminus \hat{\mathcal{L}}} & & \\ \vdots & & \ddots & \\ [\hat{B}^m Q^m]_{\hat{\mathcal{L}}} & & & [\hat{B}^m Q^m]_{[\hat{s}_m] \setminus \hat{\mathcal{L}}} \end{array} \right)$$

and the tuple of probability measures

$$\hat{P} = \left( \begin{array}{c} [(Q^1)^\top \# \hat{P}^1]_{\hat{\mathcal{L}}} \\ [(Q^1)^\top \# \hat{P}^1]_{[\hat{s}_1] \setminus \hat{\mathcal{L}}} \\ \vdots \\ [(Q^m)^\top \# \hat{P}^m]_{[\hat{s}_m] \setminus \hat{\mathcal{L}}} \end{array} \right).$$

- 12: **return**  $(\hat{\ell}, \hat{B}, \hat{P})$ .

$$\begin{aligned} \mathcal{L}: \varepsilon_1 &\sim \overline{\text{Beta}(2, 3)}, \varepsilon_2 \sim \overline{\text{Beta}(2, 5)}, \varepsilon_3 \sim \overline{\chi_4^2}, \\ I_1: \varepsilon_4 &\sim \overline{\text{Gumbel}(0, 1)}, \varepsilon_5 \sim \overline{\text{LogNormal}(0, 1)}, \\ I_2: \varepsilon_6 &\sim \overline{\text{Weibull}(1, 2)}, \varepsilon_7 \sim \overline{\text{Exp}(0.1)}, \\ I_3: \varepsilon_8 &\sim \overline{\text{SkewNormal}(6)}, \varepsilon_9 \sim \overline{\text{SkewNormal}(12)}, \end{aligned}$$

where the overline means that each distribution is standardized to have mean 0 and variance 1. Figure 6 shows histograms of the empirical distributions.

## APPENDIX F. ADDITIONAL SIMULATION RESULTS

In our small simulation study, we make additional experiments on a similar scale as in Section 5, but with more shared nodes and less domain specific nodes. This time, we consider  $\ell = 5$  shared latent nodes and  $|I_e| = 1$  domain-specific latent

**Algorithm 4** IdentifySharedGraphEmpirical

- 
- 1: **Hyperparameters:**  $\gamma > 0$ .
  - 2: **Input:** Matrix  $B^* \in \mathbb{R}^{|V| \times \ell}$ .
  - 3: **Output:** Parameter matrix  $\hat{A} \in \mathbb{R}^{\ell \times \ell}$ .
  - 4: Remove rows  $B_{i,\mathcal{L}}^*$  with  $\|B_{i,\mathcal{L}}^*\|_2 \leq \gamma$  from the matrix  $B^*$ .
  - 5: Find tuples  $(i_k, j_k)_{k \in \mathcal{L}}$  with the smallest possible scores  $\sigma_{\min}(B_{\{i_k, j_k\}, \mathcal{L}}^*)$  such that
    - (i)  $i_k \neq j_k$  for all  $k \in \mathcal{L}$  and  $\{i_k, j_k\} \cap \{i_q, j_q\} = \emptyset$  for all  $k, q \in \mathcal{L}$  such that  $k \neq q$  and
    - (ii)  $|\sigma_{\min}(B_{\{i_k, i_q\}, \mathcal{L}}^*)| > \gamma$  for all  $k, q \in \mathcal{L}$  such that  $k \neq q$ .
  - 6: Let  $I = \{i_1, \dots, i_\ell\}$  and consider the matrix  $B_{I, \mathcal{L}}^* \in \mathbb{R}^{\ell \times \ell}$ .
  - 7: Find two permutation matrices  $R_1$  and  $R_2$  such that  $W = R_1 B_{I, \mathcal{L}}^* R_2$  is as close as possible to lower triangular. This can be measured, for example, by using  $\sum_{i < j} W_{ij}^2$ .
  - 8: Multiply each column of  $W$  by the sign of its corresponding diagonal element. This yields a new matrix  $\widetilde{W}$  with all diagonal elements positive.
  - 9: Divide each row of  $\widetilde{W}$  by its corresponding diagonal element. This yields a new matrix  $\widetilde{W}'$  with all diagonal elements equal to one.
  - 10: Compute  $\hat{A} = I - (\widetilde{W}')^{-1}$ .
  - 11: **return**  $\hat{A}$ .
- 

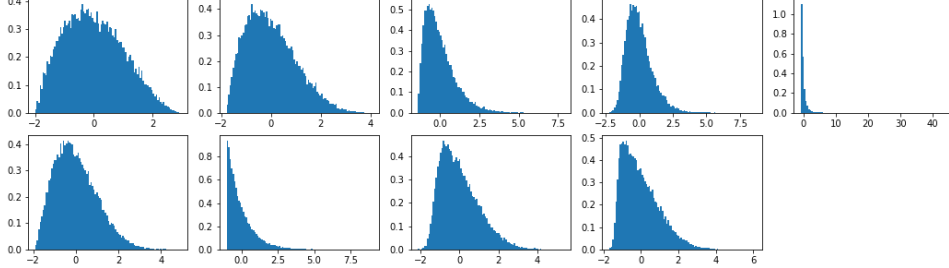


FIGURE 6. Histograms showing the frequency of 25000 values sampled from the random variables  $\varepsilon_i$  with distribution as specified in Appendix E. Each distribution has mean zero and variance one. The first row shows the empirical distributions from  $\varepsilon_1$  to  $\varepsilon_5$  and the second row from  $\varepsilon_6$  to  $\varepsilon_9$ .

node in each domain. Moreover, we also consider  $m = 4$  domains. The dimensions are given by  $d_e = d/m$  for all  $e \in [m]$  and  $d = 48$ . The graphs and edge weights are sampled equivalently as in Section 5 in the main paper. We also consider the same distribution of the error variables as specified in Appendix E, where we specify  $\mathcal{L} = \{1, 2, 3, 4, 5\}$ ,  $I_1 = \{6\}$ ,  $I_2 = \{7\}$ ,  $I_3 = \{8\}$  and  $I_4 = \{9\}$ .

Figure 7 shows the results where the scores are equivalent as in the main paper. Once again, we see that the estimation error for the matrices  $B_{\mathcal{L}}$  and  $A_{\mathcal{L}, \mathcal{L}}$  decreases with increasing sample size. This supports our proof of concept and shows that the adapted algorithms are consistent for recovering  $B_{\mathcal{L}}$  and  $A_{\mathcal{L}, \mathcal{L}}$  from finite samples.

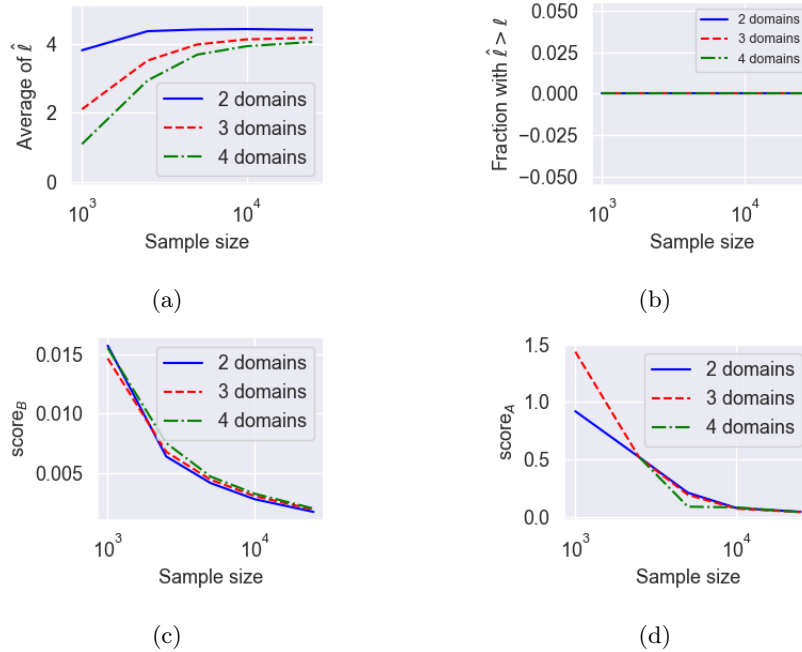


FIGURE 7. **Additional simulation results.** Logarithmic scale on the  $x$ -axis.

#### APPENDIX G. FUTURE WORK

We see many directions for future work, which include the following.

- Our work and algorithms rely on linear ICA. It would be interesting to study a more direct approach to recover the joint distribution and the causal graph. This might potentially be done by testing certain constraints implied by the model similar as the developments in the LiNGAM literature; see e.g. Shimizu et al. (2011) and Wang and Drton (2020).
- Our results require non-Gaussianity and that both the latent structural equation model and the mixing functions are linear. In non-linear setups we expect that our insights may apply and that identifiability holds only under additional assumption as in the non-linear independent component analysis literature; see e.g. Khemakhem et al. (2020) and Gresele et al. (2020). In the Gaussian case we showed in Appendix C that identifiability of the joint distribution is impossible without further assumptions on the mixing matrices  $G^e$ . However, identifiability of the joint distribution might hold under certain sparsity conditions on  $G^e$ .
- Our sufficient condition for identifiability of the shared latent graph requires two partial pure children per shared latent node. In this regard, it would also be interesting to study necessary conditions.
- It would be interesting to study the statistical properties of our setup such as theoretical bounds on the accuracy of recovering the matrices  $B$  and  $A_{\mathcal{L},\mathcal{L}}$  as well as developing algorithms that meet these bounds. Currently,

our adapted algorithms for finite samples determine the rank of a matrix by using a threshold for singular values. The algorithms depend on the choice of this parameter and it would be worth studying optimal choices. Moreover, one might consider different methods for determining the rank of a matrix.

- There might be different matching strategies of the estimated error distributions in the finite sample setting. For example, instead of matching pairwise consistently across all domains, one might find an optimal matching by solving a linear program.